NRL Report 8107

Mathematical Analysis of Circular Corrosion Cells Having Unequal Polarization Parameters

E. McCAFFERTY

Metals Performance Branch
Engineering Materials Division

Shelf
6300

August 5, 1977

NAVAL RESEARCH LABORATORY
Washington, D.C.

SECURITY CLASSIFICATION OF THIS PAGE (When Data Entered)

REPORT DOCUMENTATION PAGE		READ INSTRUCTIONS BEFORE COMPLETING FORM
1. REPORT NUMBER NRL Report 8107	2. GOVT ACCESSION NO.	3. RECIPIENT'S CATALOG NUMBER
4. TITLE (and Subtitle) MATHEMATICAL ANALYSIS OF CIRCULAR CORROSION CELLS HAVING UNEQUAL POLARIZATION PARAMETERS		5. TYPE OF REPORT & PERIOD COVERED Final report on one phase of a continuing NRL problem
		6. PERFORMING ORG. REPORT NUMBER
7. AUTHOR(s) E. McCafferty		8. CONTRACT OR GRANT NUMBER(s)
9. PERFORMING ORGANIZATION NAME AND ADDRESS Naval Research Laboratory Washington, D.C. 20375		10. PROGRAM ELEMENT, PROJECT, TASK AREA & WORK UNIT NUMBERS NRL Problem MO4-09 Project RR 022-08-44
11. CONTROLLING OFFICE NAME AND ADDRESS Office of Naval Research Arlington, Va. 22217		12. REPORT DATE August 5, 1977
		13. NUMBER OF PAGES 48
14. MONITORING AGENCY NAME & ADDRESS(if different from Controlling Office)		15. SECURITY CLASS. (of this report) UNCLASSIFIED
		15a. DECLASSIFICATION/DOWNGRADING SCHEDULE

16. DISTRIBUTION STATEMENT (of this Report)

Approved for public release; distribution unlimited

17. DISTRIBUTION STATEMENT (of the abstract entered in Block 20, if different from Report)

18. SUPPLEMENTARY NOTES

19. KEY WORDS (Continue on reverse side if necessary and identify by block number)

Corrosion
Current distribution
Potential distribution
Circular electrodes
Thin layers

20. ABSTRACT (Continue on reverse side if necessary and identify by block number)

A theoretical analysis is given for the distribution of electrode potential and current across the surface of coplanar circular galvanic cells in which the polarization parameters of the central anode and disk cathode are unequal. Central features of the model are that the electrostatic potential within the system is given by Laplace's equation and that the polarization curves of both components can be approximated by linear segments over an extended potential range. The potential distribution in a system of

(Continued)

DD FORM 1 JAN 73 1473 EDITION OF 1 NOV 65 IS OBSOLETE
S/N 0102-014-6601

SECURITY CLASSIFICATION OF THIS PAGE (When Data Entered)

(Continued)

unequal anodic and cathodic polarization parameters is not related in a simple manner to the distribution curves for equal parameters. For bulk electrolyte the value of the electrode potential across the surface depends on whether the system is under anodic, cathodic, or mixed control. The current distribution is the more uniform for combinations of more polarizable electrodes. In thin-layer electrolytes there is a geometry effect in which electrode polarization and current flow are concentrated near the anode/cathode juncture.

CONTENTS

MATHEMATICAL ANALYSIS OF CIRCULAR CORROSION CELLS HAVING UNEQUAL POLARIZATION PARAMETERS

INTRODUCTION

In many corrosion reactions the anode and cathode are spatially localized. This may occur on different surfaces, as in the galvanic corrosion of dissimilar metals, or on different parts of the same surface, as with localized geometries such as crevices. Moreover the corroding system often has a coplanar concentric circular geometry. As pointed out earlier [1, 2], examples include some instances of pitting [3], crevice corrosion under O-rings or washers [4], and corrosion under barnacles [5], under tubercules of corrosion products [6], or under dust particles in condensed moisture films [7].

In all such cases there is a potential difference between the central anode and the disk-shaped cathode surrounding it. This potential difference may arise from heterogeneities in the solid phase (such as dissimilar metals, inclusions in a base metal, or discontinuities in protective films) or from heterogeneities in the liquid phase (such as differential aeration as in crevices). Thus there is a distribution of both electrode potential and local current density as one moves radially from the center of the anode out toward the far edge of the cathode.

Gal-Or, Raz, and Yahalom [8] have mathematically treated systems of coplanar concentric circular corrosion cells. These authors analyzed the effect of various system parameters on the total current, and more recently McCafferty [1, 2] has evaluated the distribution of potential and current across such cells. These treatments essentially extended to cylindrical geometries the model developed by Waber and coworkers [9-12] in a series of publications treating semi-infinite parallel electrodes.

Two central features in the Waber model are that the anode and cathode obey linear polarization kinetics over an extended potential range and that the anodic and cathodic slopes are equal. Whereas the first assumption often holds in experiments, the second assumption rarely holds, because the anode is generally far less polarizable than the cathode.

The case of unequal anodic and cathodic linear polarization has been solved recently by Kennard and Waber [13] for semi-infinite strips of parallel electrodes under bulk electrolyte.

This report extends the Waber model of linear corrosion kinetics to circular systems with unequal polarization parameters. Equations are derived for potential and current distributions and for the total anodic current, and generalized calculations are made. Comparisons with experimental results will be made elsewhere.

Manuscript submitted February 7, 1977.

DESCRIPTION OF THE MODEL

The Corrosion Cell

The cell geometry is shown in Fig. 1. The anode and cathode outer edges are coplanar concentric circles of radii a and c respectively. The electrolyte thickness b is allowed to approach infinity for bulk electrolyte.

Linear Polarization

The cell potentials are shown in Fig. 2a, and stylized polarization curves are shown in Figs. 2b and 2c. Following Wagner [14] and Waber [9-13], an important feature of the model is that the polarization curves are linear in E vs i over an extended range. As pointed out by Kennard and Waber [13], if the plots are linear over only a portion of the curve, tangent approximations can be drawn. Thus the open-circuit potentials E_a^o and E_c^o are replaced by the intersections $E_a^{o\prime}$ and $E_c^{o\prime}$ respectively of the tangent lines with the potential axis, as shown in Fig. 2c.

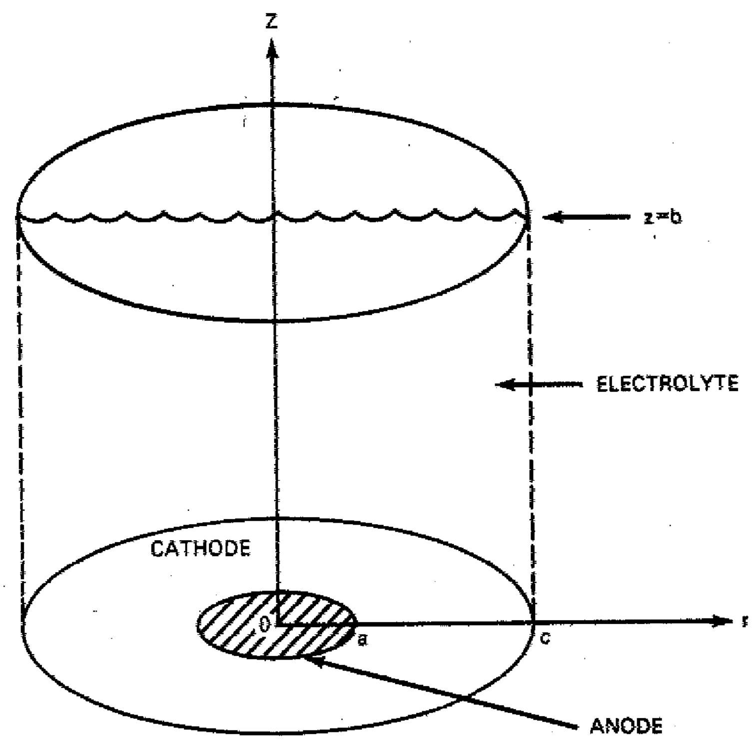

Fig. 1—The corrosion cell

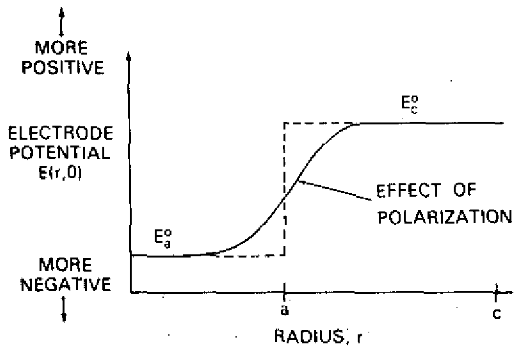

Fig. 2a—Electrode potentials across the cell. E_a^o and E_c^o refer to the open-circuit potentials of the anode and cathode respectively.

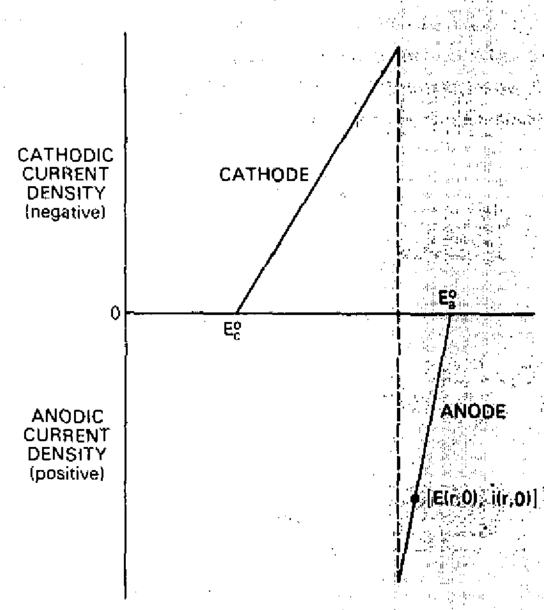

Fig. 2b—Ideal linear polarization curves over an extended potential range

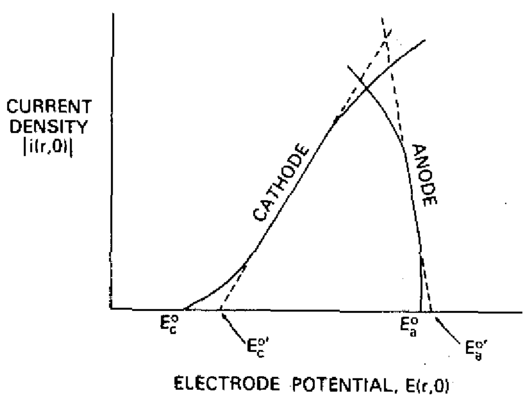

Fig. 2c—Linear approximations to the polarization curves. The extrapolated values $E_a^{o\prime}$ and $E_c^{o\prime}$ replace E_a^o and E_c^o respectively.

The linearized polarization curves are characterized by the Wagner polarization parameters

$$\mathcal{L}_a = \sigma\left|\frac{dE}{di}\right|_a \tag{1}$$

for the anode and

$$\mathcal{L}_c = \sigma\left|\frac{dE}{di}\right|_c \tag{2}$$

for the cathode, where σ is the electrolyte conductivity. The parameters $\mathcal{L}_a$ and $\mathcal{L}_c$ have the dimensions of length (cm), and $\mathcal{L}_a \neq \mathcal{L}_c$ in the present treatment.

The assumption of linear polarization over an extended potential range has been observed to be a reasonable approximation in a number of instances. For example, steels in aerated neutral to basic solutions, with or without chloride, displayed both anodic and cathodic plots which were approximately linear over an extended range [15]. Additional examples include the behavior of copper/steel couples in distilled water [16], the corrosion of tin in citrate solutions [17], and the corrosion of bare and coated aluminum in chloride solutions [18]. Other examples involve specialized geometries, such as the pitting of aluminum [19], or specialized conditions, such as the dissolution of mild steel at high anodic overpotentials in concentrated electrolytes [20]. On the cathodic side the reduction of oxygen on nickel in dilute H_2SO_4 [21] and of silver in KOH [22] display linear regions. Polarization curves for a variety of metals in thin-layer electrolytes [23] display linear regions over at least part of the potential ranges for both anodic and cathodic processes.

In some cases the linearity may be attributed predominantly to resistance polarization, caused either by iR drops through the solution or by ohmic films on the electrode surface. As pointed out by Stern and Geary [24], however, sometimes the combined effects of concentration polarization plus ohmic drops interfere with activation polarization processes so that a very short Tafel region is observed. Such cases often give straight-line segments in E vs i.

At this point it should be clear that the model invokes linearity over an *extended* potential range and not merely in the pre-Tafel region near the corrosion potential, where the usual Stern and Geary [24] linear relation is valid.

MATHEMATICAL ANALYSIS FOR BULK ELECTROLYTE

The electrostatic potential $P(x, y, z)$ is given by Laplace's equation

$$\nabla^2 P(x, y, z) = 0, \tag{3}$$

provided that there are no concentration gradients in the solution, the solution is electroneutral, and there are no sources or sinks of ions in the electrolyte [25].

With the circular geometry it is convenient to rewrite Eq. (3) in cyclindrical coordinates using the usual transformations $x = r\cos\theta$ and $y = r\sin\theta$. The result is

$$\frac{\partial^2 P(r, z)}{\partial r^2} + \frac{1}{r}\frac{\partial P(r, z)}{\partial r} + \frac{\partial^2 P(r, z)}{\partial z^2} = 0, \tag{4}$$

where the potential P is independent of the angle θ. The general approach is to solve for $P(r, z)$ in Eq. (4) subject to appropriate boundary conditions and then to evaluate the local current density $i(r, 0)$ from Ohm's law for electrolytes:

$$i(r, 0) = -\sigma\left[\frac{\partial P(r, z)}{\partial z}\right]_{z=0}, \tag{5}$$

where σ is the electrolyte conductivity.

Boundary Conditions

The boundary conditions have been discussed in some detail in a previous report [1]. In brief there is no current flow across the symmetry line $r = 0$, nor across the cathode outer boundary $r = c$. Thus

$$\left[\frac{\partial P(r, z)}{\partial r}\right]_{r=0} = 0 \tag{6}$$

and

$$\left[\frac{\partial P(r, z)}{\partial r}\right]_{r=c} = 0. \tag{7}$$

Also, the potential must be bounded at the upper physical boundary of the electrolyte, so that

$$\lim_{z\to\infty} P(r, z) < M, \tag{8}$$

where M is some finite number.

The general solution to Eq. (4) subject to the boundary conditions of Eqs. (6) through (8) is [1, 2, 8]

$$P(r, z) = C_0 + \sum_{n=1}^{\infty} C_n J_0(\lambda_n r) e^{-\lambda_n z}, \tag{9}$$

where C_0 and C_n are coefficients to be evaluated later, J_0 is the Bessel function of order zero, and $\lambda_n = x_n/c$, in which the x_n are the zeros of $J_1(x) = 0$.

Linear Polarization

The remaining boundary condition relates the electrode potential $E(r, 0)$ along the metal surface vs some standard reference electrode to the electrostatic potential $P(r, 0)$ within the electrolyte but "just outside" [26] the electrode surface. If E_a and E_c are the potentials of the polarized anode and cathode respectively, at any current density, then

$$V' - P(r, 0) = E(r, 0), \tag{10}$$

where V' is a constant which includes the various differences in electrostatic potential across the extra interfaces introduced in the measurement of a potential difference across the metal/solution interface of interest [27]. Equation (10) is developed in Appendix A.

For the anodic branch in Fig. 2b,

$$\text{slope} = \frac{i(r, 0) - 0}{E(r, 0) - E_a^o} = \left|\frac{di}{dE}\right|_a, \tag{11}$$

which after rearranging becomes

$$E(r, 0) = E_a^o + i(r, 0)\left|\frac{dE}{di}\right|_a. \tag{12}$$

Substitution of Eq. (5) in Eq. (12) gives

$$E(r, 0) = E_a^o - \sigma\left|\frac{dE}{di}\right|_a \left[\frac{\partial P(r, z)}{\partial z}\right]_{z=0} \tag{13}$$

Use of the Wagner polarization parameter as defined in Eq. (1) gives:

$$E(r, 0) = E_a^o - \mathcal{L}_a\left[\frac{\partial P(r, z)}{\partial z}\right]_{z=0}. \tag{14}$$

Substitution of Eq. (14) in Eq. (10) gives

$$P(r, 0) - \mathcal{L}_a\left[\frac{\partial P(r, z)}{\partial z}\right]_{z=0} = V' - E_a^o, \quad 0 \leqslant r < a. \tag{15a}$$

A similar expression holds for the cathode:

$$P(r, 0) - \mathcal{L}_c\left[\frac{\partial P(r, z)}{\partial z}\right]_{z=0} = V' - E_c^o, \quad a < r \leqslant c. \tag{15b}$$

Equations (15a) and (15b) are the final boundary conditions required. The indeterminate constant V' will vanish in the final forms of the expressions to be derived but will be carried along for mathematical completeness.

Evaluation of the Coefficients C_n

The boundary conditions in Eqs. (15a) and (15b) are used to determine the coefficients C_n appearing in Eq. (9). The approach is to evaluate Eqs. (15a) and (15b) using the general expression for $P(r, z)$ and then to solve the two simultaneous equations. The reader wishing to avoid the mathematical details can skip to Eq. (35).

The general expression for $P(r, z)$ was given earlier by Eq. (9). Use of Eq. (9) in (15a) gives

$$C_0 + \sum_{n=1}^{\infty} C_n(1 + \mathcal{L}_a\lambda_n)J_0(\lambda_n r) = V' - E_a^o, \quad 0 \leqslant r < a. \tag{16}$$

If this equation is multiplied through by $rJ_0(\lambda_m r)$ and integrated over the domain of applicability (from $r = 0$ to $r = a$), then

$$C_0 \int_{r=0}^{a} rJ_0(\lambda_m r)\,dr + \int_{r=0}^{a} \sum_{n=1}^{\infty} C_n(1 + \mathcal{L}_a\lambda_n)rJ_0(\lambda_n r)J_0(\lambda_m r)\,dr$$

$$= (V' - E_a^o)\int_{r=0}^{a} rJ_0(\lambda_m r)\,dr. \tag{17}$$

The first and third integrals can be evaluated from a standard recursion formula for Bessel functions [28]; that is

$$\frac{d}{dx}\left[xJ_1(x)\right] = xJ_0(x), \tag{18}$$

which, upon appropriate variable change and integration, gives

$$\int rJ_0(\lambda r)\,dr = \frac{1}{\lambda} rJ_1(\lambda r). \tag{19}$$

The second integral to be called I_2, is

$$I_2 \equiv \int_{r=0}^{a} \sum_{n=1}^{\infty} C_n(1 + \mathcal{L}_a\lambda_n)rJ_0(\lambda_n r)J_0(\lambda_m r)\,dr \tag{20}$$

or

$$I_2 = \sum_{n=1}^{\infty} C_n(1 + \mathcal{L}_a\lambda_n) \int_{r=0}^{a} rJ_0(\lambda_n r)J_0(\lambda_m r)\,dr. \tag{21}$$

The summation can be split into two cases: $n = m$, and $n \neq m$. Thus

$$I_2 = C_m(1 + \mathcal{L}_a\lambda_m) \int_{r=0}^{a} rJ_0^2(\lambda_m r)\,dr$$

$$+ \sum_{\substack{n=1 \\ n\neq m}}^{\infty} C_n(1 + \mathcal{L}_a\lambda_n) \int_{r=0}^{a} rJ_0(\lambda_n r)J_0(\lambda_m r)\,dr. \tag{22}$$

Substitution of Eqs. (19) and (22) back into Eq. (17) thus yields

$$C_0 \frac{1}{\lambda_m} aJ_1(\lambda_m a) + C_m(1 + \mathcal{L}_a\lambda_m) \int_{r=0}^{a} rJ_0^2(\lambda_m r)\,dr$$

$$+ \sum_{\substack{n=1 \\ n\neq m}}^{\infty} C_n(1 + \mathcal{L}_a\lambda_n) \int_{r=0}^{a} rJ_0(\lambda_n r)J_0(\lambda_m r)\,dr$$

$$= (V' - E_a^o) \frac{1}{\lambda_m} aJ_1(\lambda_m a). \tag{23}$$

The second integral in Eq. (23) is a Lommel integral [29]:

$$(\alpha^2 - \beta^2) \int_{x_1}^{x_2} xJ_n(\alpha x)J_n(\beta x)\,dx = \Big[x\{\beta J_n(\alpha x)J_n'(\beta x) - \alpha J_n'(\alpha x)J_n(\beta x)\}\Big]_{x_1}^{x_2} \tag{24}$$

where the primes denote differentiation with respect to the whole argument and not just x. Thus, when $n \neq m$,

$$\int_0^a rJ_0(\lambda_n r)J_0(\lambda_m r)\,dr = \frac{a}{\lambda_n^2 - \lambda_m^2} [\lambda_n J_1(\lambda_n a)J_0(\lambda_m a) - \lambda_m J_0(\lambda_n a)J_1(\lambda_m a)]. \tag{25}$$

When $n = m$, the integral becomes $\int rJ_0^2(\lambda_m r)\,dr$, which is the remaining integral to be evaluated in Eq. (23). However, when $n = m$, the right-hand side of Eq. (25) gives 0/0, so that l'Hospital's rule must be used. In this case the numerator and denominator are differentiated with respect to λ_n, and then λ_n is allowed to approach λ_m. The result (omitting several steps) is

$$\int_{r=0}^{a} rJ_0^2(\lambda_m r)\,dr = \frac{a^2}{2}\,[J_0^2(\lambda_m a) + J_1^2(\lambda_m a)]. \tag{26}$$

Use of Eqs. (25) and (26) in Eq. (23) gives

$$C_0 \frac{1}{\lambda_m} aJ_1(\lambda_m a) + C_m(1 + \mathcal{L}_a \lambda_m)\frac{a^2}{2}\,[J_0^2(\lambda_m a) + J_1^2(\lambda_m a)]$$

$$+ \sum_{\substack{n=1\\ n\neq m}}^{\infty} C_n(1 + \mathcal{L}_a\lambda_n)\frac{a}{\lambda_n^2 - \lambda_m^2}\,[\lambda_n J_1(\lambda_n a)J_0(\lambda_m a) - \lambda_m J_0(\lambda_n a)J_1(\lambda_m a)]$$

$$= (V' - E_a^o)\,\frac{a}{\lambda_m}\,J_1(\lambda_m a). \tag{27}$$

Equation (27) is one of the two simultaneous equations to be solved for the set C_n. The second equation follows from the boundary condition on the cathode given in Eq. (15b). The approach is the same as has just been completed. $P(r, 0)$ and $\partial P(r, z)/\partial z$ at $z = 0$ are evaluated from Eq. (9), so that Eq. (15b) becomes

$$C_0 + \sum_{n=1}^{\infty} C_n(1 + \mathcal{L}_c\lambda_n)J_0(\lambda_n r) = V' - E_c^o, \quad a < r \leqslant c. \tag{28}$$

Again the equation is multiplied by $rJ_0(\lambda_m r)\,dr$ and integrated over the appropriate limits, which in this case are from $r = a$ to $r = c$:

$$C_0 \int_{r=a}^{c} rJ_0(\lambda_m r)\,dr + \int_{r=a}^{c} \sum_{n=1}^{\infty} C_n(1 + \mathcal{L}_c\lambda_n) rJ_0(\lambda_n r)J_0(\lambda_m r)\,dr$$

$$= (V' - E_c^o) \int_{r=a}^{c} rJ_0(\lambda_m r)\,dr. \tag{29}$$

The first and third integrals can be evaluated using Eq. (19):

$$\frac{C_0}{\lambda_m}\,[cJ_1(\lambda_m c) - aJ_1(\lambda_m a)] + \sum_{n=1}^{\infty} C_n(1 + \mathcal{L}_c\lambda_n) \int_{r=a}^{c} rJ_0(\lambda_n r)J_0(\lambda_m r)\,dr$$

$$= \frac{V' - E_c^o}{\lambda_m}\,[cJ_1(\lambda_m c) - aJ_1(\lambda_m a)]. \tag{30}$$

By definition $\lambda_m c = x_m$ and $J_1(x_m) = 0$. Again the summation can be split into two cases, so that Eq. (30) becomes

$$-\frac{C_0}{\lambda_m} aJ_1(\lambda_m a) + C_m(1 + \mathcal{L}_c\lambda_m)\int_{r=a}^{c} rJ_0^2(\lambda_m r)\,dr$$

$$+ \sum_{\substack{n=1\\ n\neq m}}^{\infty} C_n(1 + \mathcal{L}_c\lambda_n)\int_{r=a}^{c} rJ_0(\lambda_n r)J_0(\lambda_m r)\,dr$$

$$= -\frac{(V' - E_c^o)}{\lambda_m} aJ_1(\lambda_m a). \tag{31}$$

The integrals in Eq. (31) can be evaluated as before from Eq. (24). A simpler approach is to add and subtract $\int_0^a rJ_0^2(\lambda_m r)\,dr$ to the second term and to add and subtract $\int_0^a rJ_0(\lambda_n r)J_0(\lambda_m r)\,dr$ within the summation sign: Then Eq. (31) becomes

$$-\frac{C_0}{\lambda_m} aJ_1(\lambda_m a) + C_m(1 + \mathcal{L}_c\lambda_m)\left[\int_{r=0}^{c} rJ_0^2(\lambda_m r)\,dr - \int_{r=0}^{a} rJ_0^2(\lambda_m r)\,dr\right]$$

$$+ \sum_{\substack{n=1\\ n\neq m}}^{\infty} C_n(1 + \mathcal{L}_c\lambda_n)\left[\int_{r=0}^{c} rJ_0(\lambda_n r)J_0(\lambda_m r)\,dr - \int_{r=0}^{a} rJ_0(\lambda_n r)J_0(\lambda_m r)\,dr\right]$$

$$= -\frac{(V' - E_c^o)}{\lambda_m} aJ_1(\lambda_m a). \tag{32}$$

The integrals involving the entire interval from $r = 0$ to $r = c$ are the usual orthogonality relations [30],

$$\int_{r=0}^{c} rJ_0(\lambda_n r)J_0(\lambda_m r)\,dr = \begin{cases} 0 & , n\neq m, \\ \frac{c^2}{2}\,[J_0^2(\lambda_m c)] & , n = m, \end{cases} \tag{33}$$

and the integrals from $r = 0$ to $r = a$ have already been evaluated per Eqs. (25) and (26), so that Eq. (32) reduces to

$$
-\frac{C_0}{\lambda_m} aJ_1(\lambda_m a) + C_m(1+\mathcal{L}_c\lambda_m)\left\{\frac{c^2}{2}J_0^2(\lambda_m c) - \frac{a^2}{2}\left[J_0^2(\lambda_m a) + J_1^2(\lambda_m a)\right]\right\}
$$

$$
+\sum_{\substack{n=1\\ n\neq m}}^{\infty} C_n(1+\mathcal{L}_c\lambda_n)\left\{-\frac{a}{\lambda_n^2-\lambda_m^2}\left[\lambda_n J_1(\lambda_n a)J_0(\lambda_m a) - \lambda_m J_0(\lambda_n a)J_1(\lambda_m a)\right]\right\}
$$

$$
= -\frac{(V'-E_c^o)}{\lambda_m} aJ_1(\lambda_m a). \tag{34}
$$

Equations (34) and (27) are thus two simultaneous equations in C_0 and C_n. Addition of the two equations eliminates C_0. The result, after considerable algebra, is

$$
C_m\left[\left(1+\mathcal{L}_c\frac{x_m}{c}\right)\frac{J_0^2(x_m)}{2} + (\mathcal{L}_a-\mathcal{L}_c)\left(\frac{x_m}{c}\right)\left(\frac{a}{c}\right)^2 A_m\right] + \frac{a}{c^2}(\mathcal{L}_a-\mathcal{L}_c)\sum_{\substack{n=1\\ n\neq m}}^{\infty} C_n W_{nm}
$$

$$
= -\frac{(E_a^o - E_c^o)}{x_m}\left(\frac{a}{c}\right)J_1\left(x_m\frac{a}{c}\right), \tag{35}
$$

where A_m and W_{nm} are defined by

$$
A_m = \frac{1}{2}\left[J_0^2\left(x_m\frac{a}{c}\right) + J_1^2\left(x_m\frac{a}{c}\right)\right] \tag{35a}
$$

and

$$
W_{nm} = \frac{x_n^2}{x_n^2-x_m^2}\left[J_1\left(x_n\frac{a}{c}\right)J_0\left(x_m\frac{a}{c}\right) - \frac{x_m}{x_n}J_0\left(x_n\frac{a}{c}\right)J_1\left(x_m\frac{a}{c}\right)\right]. \tag{35b}
$$

Equation (35) thus generates a series of equations, say k of them, where m is fixed in turn from 1 through k. These k equations are solved simultaneously to give the coefficients C_n from $n = 1$ to k.

The indeterminate constant V' cancels out in the generation of the set of C_n. Also, when $\mathcal{L}_a = \mathcal{L}_c = \mathcal{L}$, Eqs. (35a) and (35b) reduce to the previous case [1, 2]:

$$
C_n = -\frac{(E_a^o - E_c^o)\left(\frac{a}{c}\right)J_1\left(x_n\frac{a}{c}\right)}{x_n\left(1+\mathcal{L}\frac{x_n}{c}\right)\frac{J_0^2(x_n)}{2}}, \tag{36}
$$

where the dummy variable m has been replaced by the more general n.

Evaluation of the Coefficient C_0

The remaining coefficient C_0 can be most conveniently evaluated by going back to the original pair of equations: Eqs. (16) and (28). The approach is to multiply through in both equations by rdr and then to integrate over the appropriate limits. The operations are straightforward, so that it is not necessary to detail the proof here. The resulting two equations are

$$\frac{a^2}{2} C_0 + \sum_{n=1}^{\infty} C_n(1 + \mathcal{L}_a \lambda_n) \frac{a}{\lambda_n} J_1(\lambda_n a) = (V' - E_a^o) \frac{a^2}{2} \tag{37}$$

and

$$\frac{(c^2 - a^2)}{2} C_0 - \sum_{n=1}^{\infty} C_n(1 + \mathcal{L}_c \lambda_n) \frac{a}{\lambda_n} J_1(\lambda_n a) = (V' - E_c^o)\left(\frac{c^2 - a^2}{2}\right) \tag{38}$$

Adding Eqs. (37) and (38) and solving for C_0 gives

$$C_0 = V' - \left(\frac{a}{c}\right)^2 E_a^o - \left(\frac{c^2 - a^2}{c^2}\right) E_c^o - 2\frac{a}{c^2}(\mathcal{L}_a - \mathcal{L}_c) \sum_{n=1}^{\infty} C_n J_1\left(x_n \frac{a}{c}\right). \tag{39}$$

Electrode Potential

The electrostatic potential $P(r, z)$ at any point in the electrolyte is given by Eq. (9):

$$P(r, z) = C_0 + \sum_{n=1}^{\infty} C_n J_0\left(x_n \frac{r}{c}\right) e^{-x_n z/c}. \tag{9}$$

Use of Eq. (39) for C_0 in the above gives

$$P(r, z) = V' - \left(\frac{a}{c}\right)^2 E_a^o - \left(\frac{c^2 - a^2}{c^2}\right) E_c^o - \frac{2a}{c^2}(\mathcal{L}_a - \mathcal{L}_c) \sum_{n=1}^{\infty} C_n J_1\left(x_n \frac{a}{c}\right)$$

$$+ \sum_{n=1}^{\infty} C_n J_0\left(x_n \frac{r}{c}\right) e^{-x_n z/c}. \tag{40}$$

The relationship between the electrostatic potential $P(r, 0)$ in the electrolyte near the metal surface and the electrode potential $E(r, 0)$ vs a standard reference electrode is given by Eq. (10). Use of Eq. (40) with $z = 0$ in Eq. (10) gives

$$E(r, 0) = \left(\frac{a}{c}\right)^2 E_a^o + \left(\frac{c^2 - a^2}{c^2}\right) E_c^o + \frac{2a}{c^2} (\mathcal{L}_a - \mathcal{L}_c) \sum_{n=1}^{\infty} C_n J_1\left(x_n \frac{a}{c}\right) - \sum_{n=1}^{\infty} C_n J_0\left(x_n \frac{r}{c}\right), \tag{41}$$

where the C_n are determined from Eq. (35). Again the indeterminate constant V' vanishes in the final expression.

Local Current Density

The local current density $i(r, 0)$ along the metal surface is related to the electrostatic potential $P(r, z)$ by Eq. (5). Performing the differentiation on $P(r, z)$ as given in Eq. (40) and inserting the result in Eq. (5) yields

$$\frac{i(r, 0)}{\sigma} = \frac{1}{c} \sum_{n=1}^{\infty} C_n x_n J_0\left(x_n \frac{r}{c}\right), \tag{42}$$

where again the set of C_n is determined from Eq. (35).

Total Anodic Current

The total anodic current is related to the local current density by [1, 2, 8]:

$$I_{\text{anodic}} = \int_{r=0}^{a} \int_{\theta=0}^{2\pi} i(r, 0)\, r\, dr\, d\theta \tag{43}$$

or

$$I_{\text{anodic}} = 2\pi \int_{r=0}^{a} i(r, 0)\, r\, dr \tag{44}$$

Use of Eq. (42) in (44) gives

$$I_{\text{anodic}} = \frac{2\pi\sigma}{c} \int_{r=0}^{a} \sum_{n=1}^{\infty} C_n x_n J_0\left(x_n \frac{r}{c}\right) r\, dr \tag{45}$$

or

$$I_{\text{anodic}} = \frac{2\pi\sigma}{c} \sum_{n=1}^{\infty} \int_{r=0}^{a} C_n x_n J_0\left(x_n \frac{r}{c}\right) r\, dr. \tag{46}$$

The integral can be evaluated from Eq. (19), so that the result, omitting a few steps, is

$$\frac{I_{\text{anodic}}}{\sigma} = 2\pi a \sum_{n=1}^{\infty} C_n J_1\left(x_n \frac{a}{c}\right), \tag{47}$$

where again the set of C_n is determined from Eq. (35).

MATHEMATICAL ANALYSIS FOR A THIN-LAYER ELECTROLYTE

If the electrolyte is a thin layer of height b instead of bulk liquid, the boundary condition given by Eq. (8) is replaced by the requirement that there is no current flow across the outer boundary of the electrolyte:

$$\left[\frac{\partial P(r, z)}{\partial z}\right]_{z=b} = 0. \tag{48}$$

The other boundary conditions are the same as for the bulk case. The general solution of Laplace's equation subject to the restrictions of Eqs. (6), (7), and (48) is

$$P(r, z) = C_0 + \sum_{n=1}^{\infty} C_n \cosh\left[\frac{x_n}{c}(b-z)\right] J_0\left(x_n \frac{r}{c}\right). \tag{49}$$

The coefficients C_0 and C_n are evaluated from Eqs. (15a) and (15b), as was done for the case of bulk electrolyte. The procedure is exactly the same as for the bulk case; hence only the results are listed below.

The coefficients C_n are given by the systems of simultaneous equations

$$C_m\left\{\left[1 + \mathcal{L}_c \frac{x_m}{c} \tanh\left(x_m \frac{b}{c}\right)\right] \frac{J_0^2(x_m)}{2} + (\mathcal{L}_a - \mathcal{L}_c)\frac{x_m}{c}\left(\frac{a}{c}\right)^2 \tanh\left(x_m \frac{b}{c}\right) A_m\right\}$$

$$+ \frac{a}{c^2} \frac{(\mathcal{L}_a - \mathcal{L}_c)}{\cosh\left(x_m \frac{b}{c}\right)} \sum_{\substack{n=1 \\ n \neq m}}^{\infty} C_n W_{nm} \sinh\left(x_n \frac{b}{c}\right) = -\frac{1}{\cosh\left(x_m \frac{b}{c}\right)} \frac{(E_a^o - E_c^o)}{x_m} \left(\frac{a}{c}\right) J_1\left(x_m \frac{a}{c}\right), \tag{50}$$

where again A_m and W_{nm} are defined by Eqs. (35a) and (35b) respectively and m takes on the values 1 through k successively.

The constant C_0 is given by

$$C_0 = V' - \left(\frac{a}{c}\right)^2 E_a^o - \left(\frac{c^2 - a^2}{c^2}\right) E_c^o - \frac{2a}{c^2} \; (\mathcal{L}_a - \mathcal{L}_c) \sum_{n=1}^{\infty} C_n \sinh\left(x_n \frac{b}{c}\right) J_1\left(x_n \frac{a}{c}\right), \tag{51}$$

and

$$E(r, 0) = \left(\frac{a}{c}\right)^2 E_a^o + \left(\frac{c^2 - a^2}{c^2}\right) E_c^o + \frac{2a}{c^2} \; (\mathcal{L}_a - \mathcal{L}_c) \sum_{n=1}^{\infty} C_n \sinh\left(x_n \frac{b}{c}\right) J_1\left(x_n \frac{a}{c}\right)$$

$$- \sum_{n=1}^{\infty} C_n \cosh\left(x_n \frac{b}{c}\right) J_0\left(x_n \frac{r}{c}\right). \tag{52}$$

The local current density is given by

$$\frac{i(r, 0)}{\sigma} = \frac{1}{c} \sum_{n=1}^{\infty} C_n x_n \sinh\left(x_n \frac{b}{c}\right) J_0\left(x_n \frac{r}{c}\right), \tag{53}$$

and the total anodic current is

$$\frac{I_{\text{anodic}}}{\sigma} = 2\pi a \sum_{n=1}^{\infty} C_n \sinh\left(x_n \frac{b}{c}\right) J_1\left(x_n \frac{a}{c}\right). \tag{54}$$

When $b \rightarrow \infty$, C_n (thin-layer) $\times \sinh(x_n b/c) \rightarrow C_n$ (bulk), so that the expressions for thin-layer electrolyte reduce to the corresponding equations for a bulk electrolyte for large b.

The various expressions for the thin-layer and bulk cases are summarized in Table 1.

PREVIOUS CASE OF EQUAL POLARIZATION PARAMETERS

When $\mathcal{L}_a = \mathcal{L}_c = \mathcal{L}$, the preceding results for bulk and thin-layer electrolytes reduce to

$$E(r, 0) = \left(\frac{a}{c}\right)^2 E_a^o + \left(\frac{c^2 - a^2}{c^2}\right) E_c^o$$

$$+ 2\left(\frac{a}{c}\right)(E_a^o - E_c^o) \sum_{n=1}^{\infty} \frac{J_1\left(x_n \frac{a}{c}\right)}{x_n\left[1 + \mathcal{L} \frac{x_n}{c} Q\right] J_0^2(x_n)} J_0\left(x_n \frac{r}{c}\right), \tag{55}$$

Table 1—Summary of Relationships for Coplanár Circular Electrodes under a Bulk and a Thin-Layer Electrolyte. The hyperbolic functions in the upper part of the brackets apply to thin layers, and are replaced by 1 for a bulk electrolyte. The numbers in parentheses refer to equation numbers in the text.

Coefficients C_n

$$
\begin{aligned}
C_m\Bigg[&\left[1 + \mathcal{L}_c \frac{x_m}{c}\left\{\begin{matrix}\tanh\left(x_m \dfrac{b}{c}\right) \\ \text{or} \\ 1\end{matrix}\right\}\right]\frac{J_0^2(x_m)}{2} \\
&+ (\mathcal{L}_a - \mathcal{L}_c)\frac{x_m}{c}\left(\frac{a}{c}\right)^2\left[\frac{J_0^2\left(x_m \frac{a}{c}\right) + J_1^2\left(x_m \frac{a}{c}\right)}{2}\right]\left\{\begin{matrix}\tanh\left(x_m \dfrac{b}{c}\right) \\ \text{or} \\ 1\end{matrix}\right\}\Bigg] \\
&+ \frac{a}{c^2}\,\frac{\mathcal{L}_a - \mathcal{L}_c}{\left\{\begin{matrix}\cosh\left(x_m \dfrac{b}{c}\right) \\ \text{or} \\ 1\end{matrix}\right\}}\sum_{\substack{n=1 \\ n \neq m}}^{\infty} C_n \left\{\begin{matrix}\sinh\left(x_n \dfrac{b}{c}\right) \\ \text{or} \\ 1\end{matrix}\right\}\frac{x_n^2}{x_n^2 - x_m^2}\Bigg[J_1\left(x_n \frac{a}{c}\right)J_0\left(x_m \frac{a}{c}\right) \\
&- \frac{x_m}{x_n} J_0\left(x_n \frac{a}{c}\right) J_1\left(x_m \frac{a}{c}\right)\Bigg] = -\frac{1}{\left\{\begin{matrix}\cosh\left(x_m \dfrac{b}{c}\right) \\ \text{or} \\ 1\end{matrix}\right\}}\frac{(E_a^o - E_c^o)}{x_m}\,\frac{a}{c}\,J_1\left(x_m \frac{a}{c}\right). \qquad (35, 50)
\end{aligned}
$$

Electrode Potential

$$
\begin{aligned}
E(r, 0) = &\left(\frac{a}{c}\right)^2 E_a^o + \left(\frac{c^2 - a^2}{c^2}\right)E_c^o + \frac{2a}{c^2}(\mathcal{L}_a - \mathcal{L}_c)\sum_{n=1}^{\infty} C_n \left\{\begin{matrix}\sinh\left(x_n \dfrac{b}{c}\right) \\ \text{or} \\ 1\end{matrix}\right\} J_1\left(x_n \frac{a}{c}\right) \\
&- \sum_{n=1}^{\infty} C_n \left\{\begin{matrix}\cosh\left(x_n \dfrac{b}{c}\right) \\ \text{or} \\ 1\end{matrix}\right\} J_0\left(x_n \frac{r}{c}\right). \qquad (41, 52)
\end{aligned}
$$

Local Current Density

$$
\frac{i(r, 0)}{\sigma} = \frac{1}{c}\sum_{n=1}^{\infty} C_n x_n \left\{\begin{matrix}\sinh\ x_n \dfrac{b}{c} \\ \text{or} \\ 1\end{matrix}\right\} J_0\left(x_n \frac{r}{c}\right) \qquad (42, 53)
$$

Total Anodic Current

$$
\frac{I_{\text{anodic}}}{\sigma} = 2\pi a \sum_{n=1}^{\infty} C_n \left\{\begin{matrix}\sinh\left(x_n \dfrac{b}{c}\right) \\ \text{or} \\ 1\end{matrix}\right\} J_1\left(x_n \frac{a}{c}\right) \qquad (47, 54)
$$

$$\frac{i(r,0)}{\sigma} = -2\frac{a}{c^2}\,(E_a^o - E_c^o)\sum_{n=1}^{\infty}\frac{J_1\left(x_n\frac{a}{c}\right)Q}{\left[1 + \mathcal{L}\frac{x_n}{c}Q\right]J_0^2(x_n)}\,J_0\left(x_n\frac{r}{c}\right), \tag{56}$$

and:

$$\frac{I_{\text{anodic}}}{\sigma} = -4\pi\frac{a^2}{c}\,(E_a^o - E_c^o)\sum_{n=1}^{\infty}\frac{J_1^2\left(x_n\frac{a}{c}\right)Q}{x_n\left[1 + \mathcal{L}\frac{x_n}{c}Q\right]J_0^2(x_n)}, \tag{57}$$

where in each of the above

$$Q = \begin{cases} 1, & \text{bulk electrolyte,} \\ \tanh\left(x_n\frac{b}{c}\right), & \text{thin layer.} \end{cases} \tag{58}$$

These equations are the same as those previously reported except that the signs of electrode potentials in Eqs. (55) through (57) now conform to the convention that the noble direction is the more positive.

NUMERICAL EVALUATION

Values of $\mathcal{L}_a$ and $\mathcal{L}_c$

In general the anode and cathode have different polarizabilities (the two electrode potentials respond differently to the passage of current). In many instances the anode is the less polarizable. This is illustrated by many electrode kinetic studies carried out under carefully controlled conditions. With iron, for example, in a variety of deaerated electrolytes, anodic Tafel slopes of 30 to 80 mV/decade have been observed, while the cathodic slopes were 120 mV/decade [31-34]. Other metals in the iron group (nickel and cobalt) have been observed to behave similarly [35].

To cite two more examples, cadmium undergoes self-dissolution to Cd^{+2} in acids by two consecutive single-electron transfer reactions, and indium goes to In^{+3} through three consecutive single-electron transfers. The observed anodic Tafel slopes are 40 to 50mV/decade (0°C) for cadmium [36] and 22 mV/decade for indium [37], in good correspondence with the theoretical values of 2.303 RT/(3/2)F and 2.303 RT/(5/2)F respectively. The hydrogen-evolution reaction on both surfaces gave cathodic Tafel slopes of 115 mV/decade and 120 mV/decade respectively, indicative of a single-electron transfer characterized by a theoretical value of 2.303 RT/(1/2)F.

In more practical situations where conditions are not as well defined, Tafel behavior is not always observed, but instead polarization curves sometimes display segments which are approximately linear in current (rather than the logarithm of current) over a considerable potential range, as discussed earlier. In these instances the cathode often again is the more polarizable. Figure 3a shows a schematic Evans diagram [38] for a bimetallic couple under cathodic control. Other possibilities, however, include anodic control (Fig. 3b) and mixed control (Fig. 3c). This last case would approximate earlier treatments [1, 2, 8] for $\mathcal{L}_a = \mathcal{L}_c$.

Values of Wagner linear polarization curves compiled [1, 2] from the literature indicate that $\mathcal{L}_a$ is generally of the order of 1 to 10 cm while $\mathcal{L}_c$ is usually 10 to 100 cm, although there are exceptions. In data tabulated by Gouda and Mourad [15] for steel in a variety of neutral to basic solutions both with and without added chloride, the cathodic slope $|dE/di|$ varied from 1.5 times to approximately 20 times the anodic slope but with most ratios in the range of 5 to 10. Specific conductivities were listed for only three solutions, for which values of $\mathcal{L}_a$ are calculated to be 0.9, 1.9, and 48 cm, with corresponding $\mathcal{L}_c$ values of 7.5, 12.2, and 193 cm respectively.

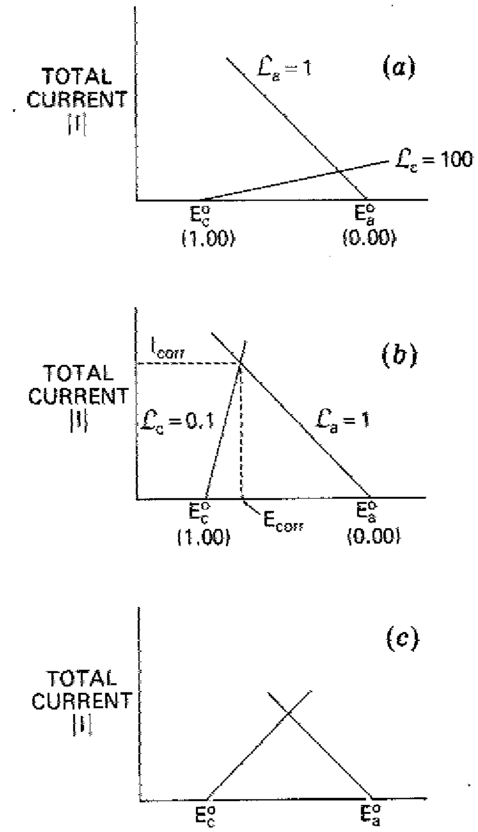

Fig. 3—Schematic representations of cathodic, anodic, and mixed control with $\mathcal{L}_a$ fixed at 1 cm in each case

Bulk Electrolyte

For the calculations in this section, the anodic polarization parameter is fixed at $\mathcal{L}_a = 1$ cm. Figure 4 shows the potential distribution $E(r, 0)$ for $\mathcal{L}_a = 1$ cm and $\mathcal{L}_c = 10$ cm for fixed values of $E_a^0 = 0.00\ V$ and $E_c^0 = 1.00\ V$. The coefficients C_n were calculated up to C_{100} using the system of simultaneous equations generated by Eq. (35). These simultaneous equations were solved using the CDC 3800 computer, and the coefficients were then substituted in Eq. (41) to obtain the electrode potential distribution. Convergence was assessed by numerical evaluation. The computer program is given in Appendix B.

Figure 4 also shows potential distribution plots for $\mathcal{L}_a = \mathcal{L}_c = 1$ cm and $\mathcal{L}_a = \mathcal{L}_c = 10$ cm, calculated from Eq. (55). It is evident that the potential behavior of the electrodes with unequal anodic and cathodic polarization parameters cannot be deduced from the two separate curves for the equal polarization parameters.

The corresponding current density curves for the three systems are shown in Fig. 5. It is seen that the values for the case of unequal parameters are intermediate between the two cases where $\mathcal{L}_a = \mathcal{L}_c = 1$ cm and $\mathcal{L}_a = \mathcal{L}_c = 10$ cm.

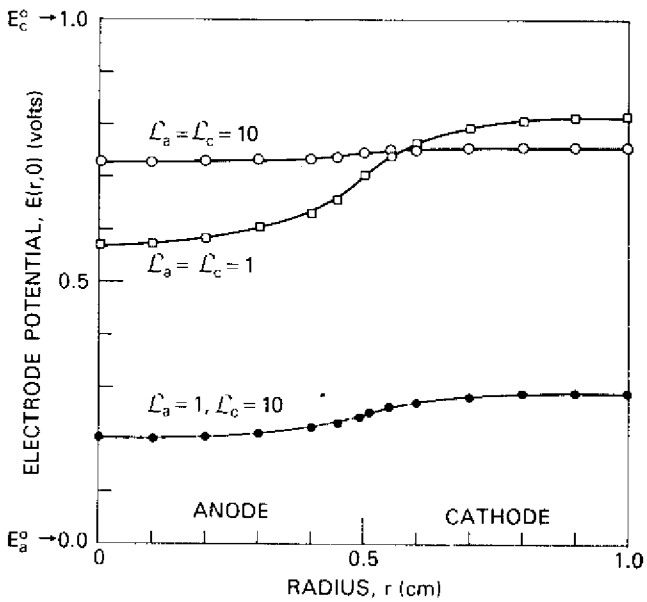

Fig. 4—Comparison of electrode potential distributions for equal and unequal polarization parameters with bulk electrolyte (anode radius $a = 0.5$ cm, cathode radius $c = 1.0$ cm, $E_a^o = 0.00\ V$, and $E_c^o = 1.00\ V$)

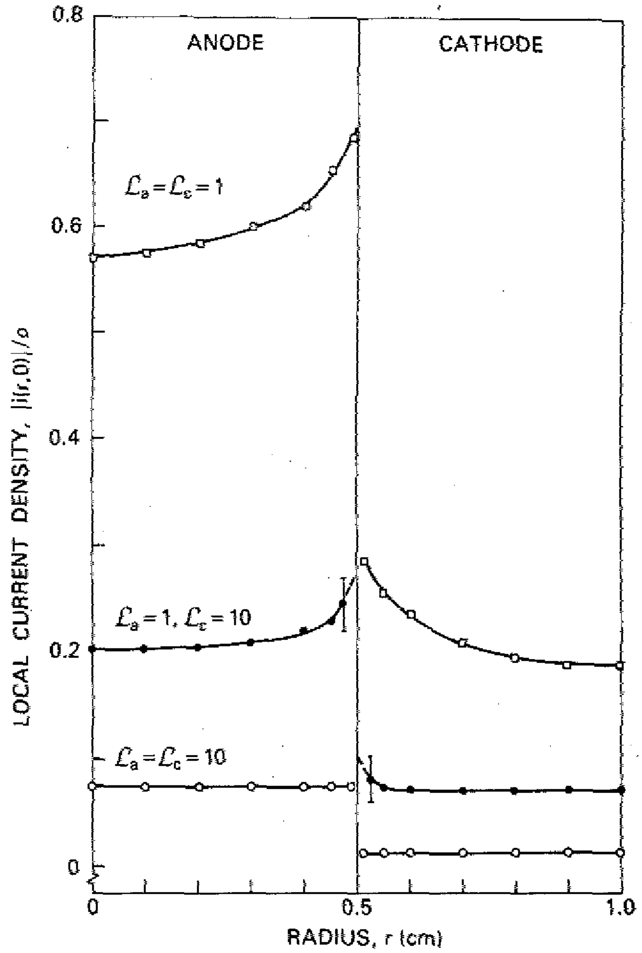

Fig. 5—Current distributions corresponding to the electrode potential distributions in Fig. 4

Figure 6 shows the potential distribution calculated from Eq. (41) with $n = 100$ for a fixed value of $\mathcal{L}_a = 1$ cm but with variable $\mathcal{L}_c$. Corresponding current distribution curves calculated from Eq. (42) are shown in Fig. 7. When $\mathcal{L}_a = 1$ cm and $\mathcal{L}_c = 0.1$ cm, the galvanic couple is under anodic control, as depicted in Fig. 3b, and the electrode potentials across the metal surface of both components are polarized up near the potential of the uncoupled cathode.

When $\mathcal{L}_c >> \mathcal{L}_a$, such as $\mathcal{L}_a = 1$ cm and $\mathcal{L}_c = 100$ cm, the system is under cathodic control, as illustrated schematically in Fig. 3a. For this case, Fig. 3a predicts that the electrode potential would approach the values of the open-circuit potential of the anode and the current would be much less than for the case of anodic control (for fixed $\mathcal{L}_a$). These expected trends are verified in the results of the numerical analysis shown in Figs. 6 and 7.

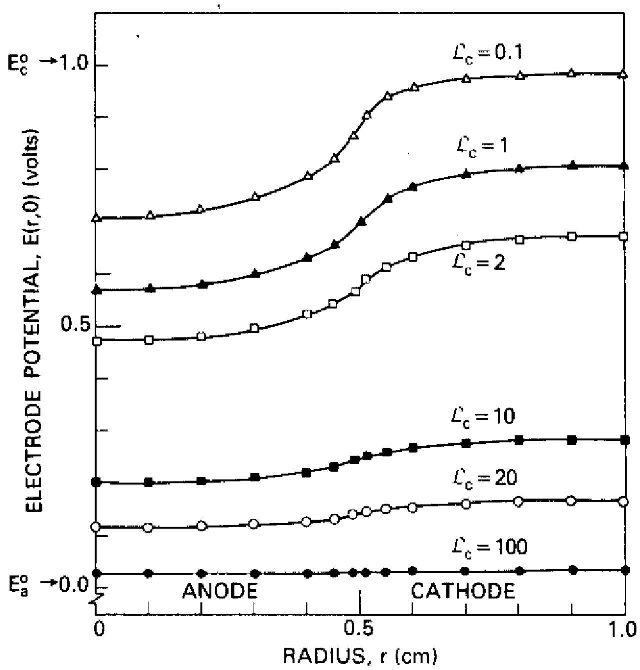

Fig. 6—Distribution of electrode potential across circular cells under bulk electrolyte with $\mathcal{L}_a$ fixed at 1 cm, combined with various values of $\mathcal{L}_c$ (anode radius a = 0.5 cm, cathode radius c = 1.0 cm, E_a^o = 0.00 V, and E_c^o = 1.00 V)

Results in Figs. 6 and 7 for $\mathcal{L}_a = \mathcal{L}_c = 1$ cm also provide a check on the consistency of the present method with the previous relationships for equal polarization parameters. Both current and potential distributions calculated from the set of C_n resulting from Eq. (35) with $\mathcal{L}_a$ and $\mathcal{L}_c$ both equal to 1 cm agree with the results obtained from Eqs. (55) and (56).

One additional trend can be seen in Figs. 6 and 7. For this system of fixed $\mathcal{L}_a$, the more polarizable the cathode (the larger $\mathcal{L}_c$), the more uniform the potential and current distribution.

The total anodic current was calculated from Eq. (47) for the systems with $\mathcal{L}_a$ fixed at 1 cm with variable $\mathcal{L}_c$. Results are listed in Table 2.

The total anodic current can also be calculated from the schematic Evans diagrams shown in Fig. 3. For the anodic branch

$$\left|\frac{dE}{dI}\right|_a = \frac{E_{corr} - E_a^o}{I_{corr}} \tag{59}$$

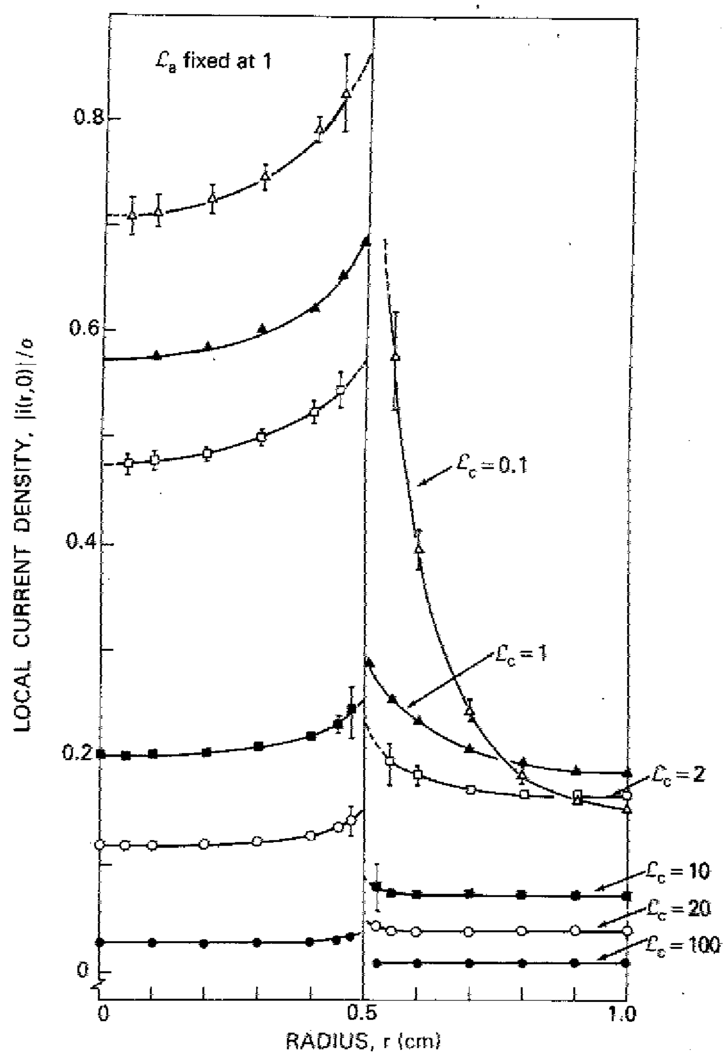

Fig. 7—Distribution of current across circular cells under bulk electrolyte with $\mathcal{L}_a$ fixed at 1 cm and combined with various values of $\mathcal{L}_c$ (anode radius a = 0.5 cm, cathode radius c = 1.0 cm, $E_a^o = 0.00$ V, and $E_c^o = 1.00$ V)

and for the cathodic branch

$$\left|\frac{dE}{dI}\right|_c = -\frac{E_{\text{corr}} - E_c^o}{I_{\text{corr}}}, \tag{60}$$

where I_{corr} is the corrosion current (the total anodic current referred to earlier as I_{anodic}). $I_a = i_a A_a$ and $I_c = i_c A_c$, where A_a and A_c are the area of anode and cathode respectively. Use of Eqs. (1) and (2) in Eqs. (59) and (60) gives

Table 2—Comparison of Total Current Calculated from Evans Diagrams and From Summation of Current Distribution Curves for Circular Couples Under Bulk Electrolyte (anode radius a = 0.5 cm, cathode radius c = 1.0 cm, E_a^o = 0.00 V, and E_c^o = 1.00 V)

$\mathcal{L}_a$ (cm)	$\mathcal{L}_c$ (cm)	I_{corr}/σ, Calculated from Evans Diagrams: Eq. (61)	I_{anodic}/σ, Calculated from Eqs. (35) and (47)
1	0.1	0.760	0.607
	1	0.589	0.485
	2	0.471	0.401
	10	0.181	0.169
	20	0.103	0.099
	50	0.0445	0.0437
	100	0.0228	0.0227
10	10	0.0589	0.0576
	100	0.0181	0.0179
100	100	0.00589	0.00589

$$\frac{I_{corr}}{\sigma} = \frac{E_c^o - E_a^o}{\dfrac{\mathcal{L}_a}{A_a} + \dfrac{\mathcal{L}_c}{A_c}}, \tag{61}$$

where again I_{corr} has the same meaning of I_{anodic} in Eq. (47).

Values of I_{anodic}/σ calculated from Eq. (47) are also listed in Table 2. These calculated values agree with the results from the computer analysis for $\mathcal{L}_a$ = 1 cm coupled with cathodic values of $\mathcal{L}_c$ = 50 cm and $\mathcal{L}_c$ = 100 cm, where the current distribution is uniform, as shown in Fig. 7. There is disagreement between the results of the Evans-diagram analysis and the computer analysis for those systems where there is a nonuniform distribution of current, and this divergence is greater the more pronounced the localized attack at the anode/cathode juncture.

Results for $\mathcal{L}_a = \mathcal{L}_c$ = 10 cm and $\mathcal{L}_a = \mathcal{L}_c$ = 100 cm are also included in Table 2. Current distribution plots published in an earlier report [1] were nearly uniform for the former system and exactly so for the latter. The current distribution for $\mathcal{L}_a$ = 10 cm and $\mathcal{L}_c$ = 100 cm was calculated from Eq. (42) and was also observed to be uniform (The plot is not shown here.) Thus there is good agreement between Evans-diagram analyses and computer calculations for the cases where there is a uniform current distribution.

Thus the classic Evans polarization diagrams cannot be used to accurately predict the value of galvanic currents unless the anode and cathode components each behave uniformly.

Thin-Layer Electrolyte

Figure 8 shows the electrode potential $E(r, 0)$ for $\mathcal{L}_a = 1$ cm and $\mathcal{L}_c = 10$ cm for different electrolyte thicknesses. The coefficients C_n were computed up to C_{100} from Eq. (50) and were used in Eq. (52) to obtain the potential distributions. The computer program for thin layers is given in Appendix C.

Figure 8 shows that the potential distribution is almost uniform for bulk electrolyte, but with thin layers most of the polarization takes place near the anode/cathode juncture. The anode center and cathode outer edge are virtually unaffected by the presence of each other for the thinnest electrolyte of 0.001 cm.

The corresponding current distributions are shown in Fig. 9. The local current densities were calculated from Eqs. (50) and (53) with $n = 100$, except near $r = 0.0$ and $r = 0.5$, where 125 terms were used. For the thin layers there is a geometry effect in which the corrosion attack is concentrated near the anode/cathode boundary.

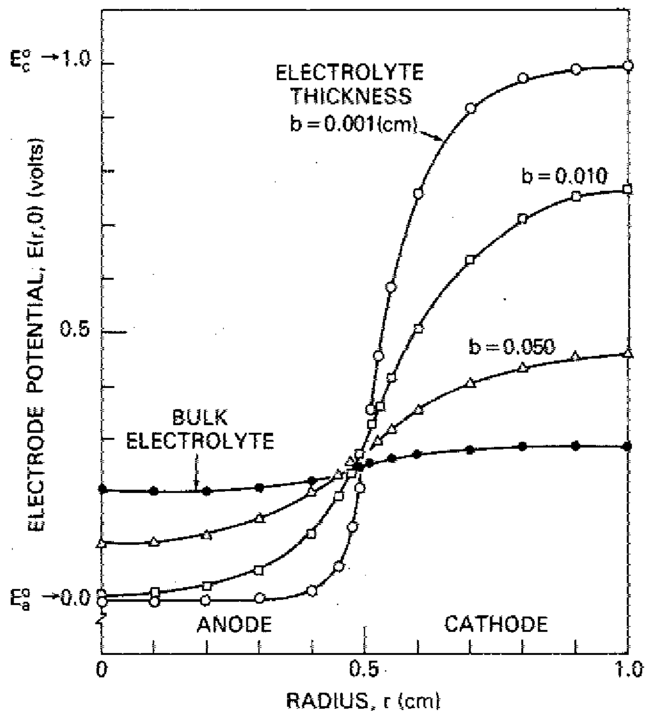

Fig. 8—Distribution of electrode potential for $\mathcal{L}_a = 1$ cm and $\mathcal{L}_c$ = 10 cm for different electrolyte thicknesses (anode radius a = 0.5 cm, cathode radius c = 1.0 cm, E_a^o = 0.00 V, and E_c^o = 1.00 V)

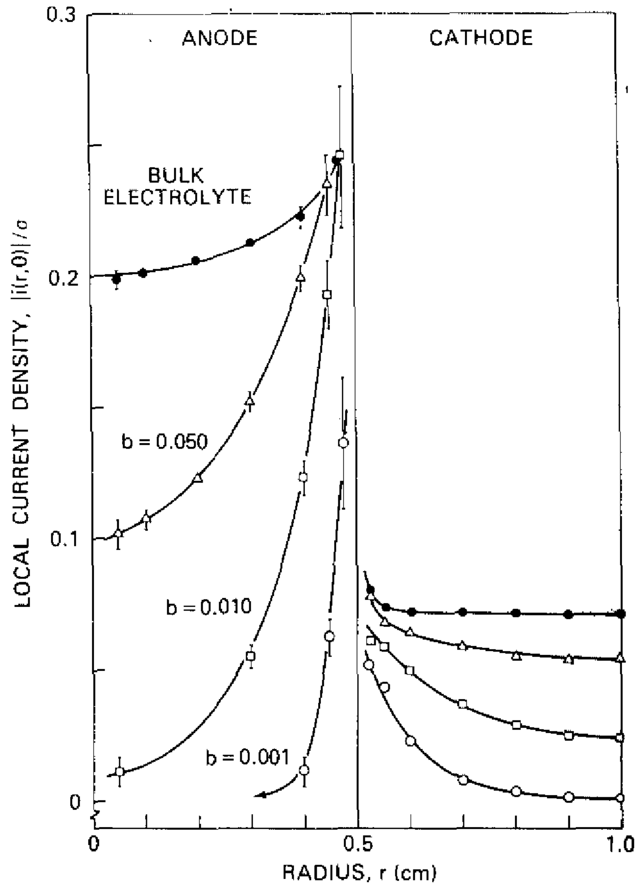

Fig. 9—Current distribution for $\mathcal{L}_a$ = 1 cm and $\mathcal{L}_c$ = 10 cm for different electrolyte thicknesses. The cell parameters are the same as in Fig. 8. (Limits between which the local current densities oscillate as computed from Eq. (53) are indicated for the anodic points. Limits are not shown for the cathode but are approximately half the range of the anodic points)

Figure 10 shows the total anodic current calculated from Eq. (54) for two different combinations of $\mathcal{L}_a$ and $\mathcal{L}_c$. In both cases the total current approaches values for the bulk for electrolyte thicknesses of approximately 0.1 to 0.3 cm.

Figure 11 compares the potential distribution for $\mathcal{L}_a$ = 1 cm and $\mathcal{L}_c$ = 10 cm to the cases of equal polarization parameters: $\mathcal{L}_a = \mathcal{L}_c$ = 1 cm and $\mathcal{L}_a = \mathcal{L}_c$ = 10 cm for an electrolyte thickness of 0.001 cm. Figure 12 shows a similar curve for $\mathcal{L}_a$ = 10 cm and $\mathcal{L}_c$ = 100 cm. In each case the potential distribution for the system of unequal parameters is not related in a simple manner to the individual distribution curves for each of the two equal parameters.

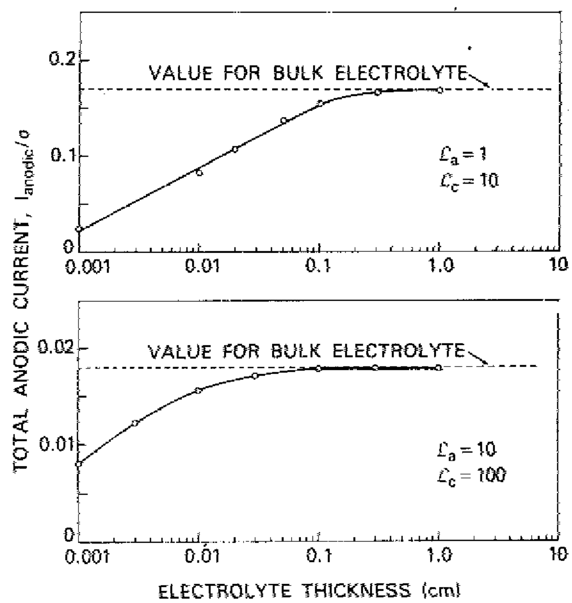

Fig. 10—Total anodic current computed as a function of electrolyte thickness for two different combinations of $\mathcal{L}_a$ and $\mathcal{L}_c$ (anode radius a = 0.5 cm, cathode radius c = 1.0 cm, E_a^o = 0.00 V, and E_c^o = 1.00 V)

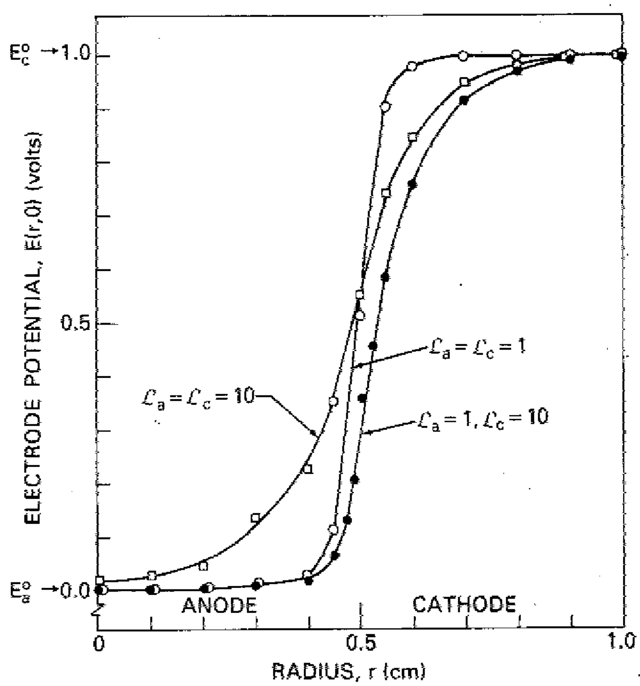

Fig. 11—Comparison of electrode potential distribution for equal and unequal polarization parameters for a thin-layer electrolyte of thickness b = 0.001 cm (anode radius a = 0.5 cm, cathode radius c = 1.0 cm, E_a^o = 0.00 V, and E_c^o = 1.00 V)

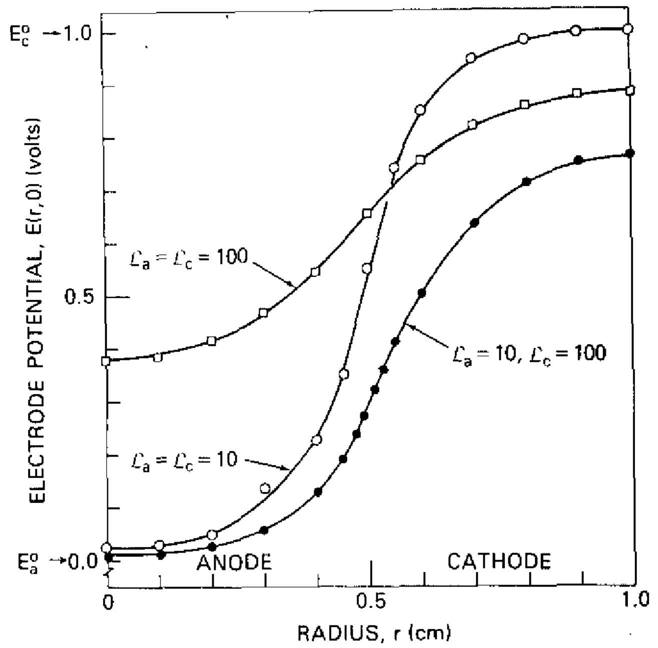

Fig. 12—A second comparison of electrode potential distribution for equal and unequal polarization parameters for a thin-layer electrolyte of thickness b = 0.001 cm (anode radius a = 0.5 cm, cathode radius c = 1.0 cm, E_a^o = 0.00 V, and E_c^o = 1.00 V)

SUMMARY

A mathematical model has been developed to describe the distribution of potential and current across circular corrosion cells having unequal anodic and cathodic linear polarization parameters. This analysis is applicable to systems of dissimilar-metal galvanic couples or to systems with a localized geometry effect, as in pitting corrosion.

The potential distribution in a system having unequal anodic and cathodic polarization parameters is not related in a simple manner to the separate distribution curves for the two cases where the polarization parameters are equal.

For bulk electrolyte the value of the electrode potentials depends on whether the system is under anodic, cathodic, or mixed control. Current distribution is more uniform for the more polarizable combinations of electrodes. Thus the total corrosion current calculated from the Evans diagram is in error if the individual current distributions are not uniform.

In thin-layer electrolytes there is a geometry effect in which the electrode polarization and current flow is concentrated near the anode/cathode juncture. In a typical system the tendency toward bulk behavior occurs at about 0.1 to 0.3 cm (1000 to 3000 μm).

REFERENCES

1. E. McCafferty, "Mathematical Analysis of Current Distribution in Corrosion Cells with Circular Geometry," NRL Report 7835, Jan. 31, 1975.
2. E. McCafferty, Corrosion Sci. 16, 183 (1976).
3. K.J. Vetter and H. Strehblow, p. 240, in "Localized Corrosion," NACE, Houston, Texas, 1974.
4. B.F. Brown, Machine Design 40 (2), 165 (1968).
5. F.L. LaQue, *Marine Corrosion*, Wiley-Interscience, New York, 1975, p. 117.
6. A. Cohen and W.S. Lyman, Materials Protection and Protection 11 (2), 48 (1972).
7. I.L. Rozenfeld, "Atmospheric Corrosion of Metals," NACE, Houston, Texas, 1972, p. 121.
8. L. Gal-Or, Y. Raz, and J. Yahalom, J. Electrochem. Soc. 120, 598 (1973).
9. J.T. Waber, J. Electrochem. Soc. 101, 271 (1954).
10. J.T. Waber and M. Rosenbluth, J. Electrochem. Soc. 102, 344 (1955).
11. J.T. Waber, J. Electrochem. Soc. 102, 420 (1955).
12. J.T. Waber and B. Fagan, J. Electrochem. Soc. 103, 64 (1956).
13. K. Kennard and J.T. Waber, J. Electrochem. Soc. 117, 880 (1970).
14. C. Wagner, J. Electrochem. Soc. 98, 116 (1951).
15. V.K. Gouda and H.M. Mourad, Corrosion Sci. 14, 681 (1974); 15, 307 (1975); 15, 317 (1975); and 15, 329 (1975).
16. T.K. Ross and B.P.L. Hitchen, Corrosion Sci. 1, 65 (1961)
17. P.W. Board, R.V. Holland, and D. Britz, British Corrosion J. 3, 238 (1968).
18. P.L. Bonora, A. Barbangelo, and G.P. Ponzano, British Corrosion J. 10, 23 (1975).
19. B.N. Stirrup, N.A. Hampson, and I.S. Midgley, J. Applied Electrochem. 5, 229 (1975).
20. K.W. Mao, J. Electrochem. Soc. 120, 1056 (1973).
21. J. Postlethwaite and D.R. Hurp, Corrosion Sci. 7, 435 (1967).
22. I. Marcos, J. Electrochem. Soc. 122, 1008 (1975).
23. I.L. Rozenfeld, pp. 60-90 in Ref. 7.
24. M. Stern and A.L. Geary, J. Electrochem. Soc. 104, 56 (1957).
25. J. Newman, p. 87, in *Advances in Electrochemistry and Electrochemical Engineering*, C.W. Tobias, editor, Vol. 5, Interscience, New York, 1967.
26. D.C. Grahame, Chem. Revs. 41, 441 (1947).
27. J. O'M. Bockris and A.K.N. Reddy, *Modern Aspects of Electrochemistry*, Vol. 2, Plenum Press, New York, 1970, pp. 644 ff.

28. F.E. Relton, *Applied Bessel Functions*, Dover, New York, 1965. p. 79.

29. F.E. Relton, p. 51 in Ref. 28.

30. H.F. Davis, *Fourier Series and Orthogonal Functions*, Allyn and Bacon, Boston, 1963, p. 240.

31. E.J. Kelly, J. Electrochem. Soc. 112, 124 (1965).

32. S. Asakura and K. Nobe, J. Electrochem. Soc. 118, 13 (1971) and 118, 19 (1971).

33. F. Hilbert, Y. Miyoshi, G. Eichkorn, and W.J. Lorenz, J. Electrochem. Soc. 118, 1919 (1971).

34. E. McCafferty and N. Hackerman, J. Electrochem. Soc. 119, 999 (1972).

35. References cited in Ref. 33.

36. K.E. Heusler and L. Gaiser, J. Electrochem. Soc. 117, 762 (1970).

37. C.K. Watanabe and K. Nobe, J. Applied Electrochem. 6, 159 (1976).

38. U.R. Evans, *Metallic Corrosion, Passivity, and Protection*, Arnold, London, 1948.

Appendix A

RELATIONSHIP BETWEEN THE ELECTRODE POTENTIAL AND THE ELECTROSTATIC POTENTIAL AT THE METAL/SOLUTION INTERFACE

As pointed out by Bockris and Reddy [A1], it is impossible to measure the electrode potential of a metal/solution interface without introducing additional extraneous interfaces during the measurement process. This is illustrated in Fig. A1, where the electrode potentials of the coplanar anode and cathode are to be measured versus the reference electrode.

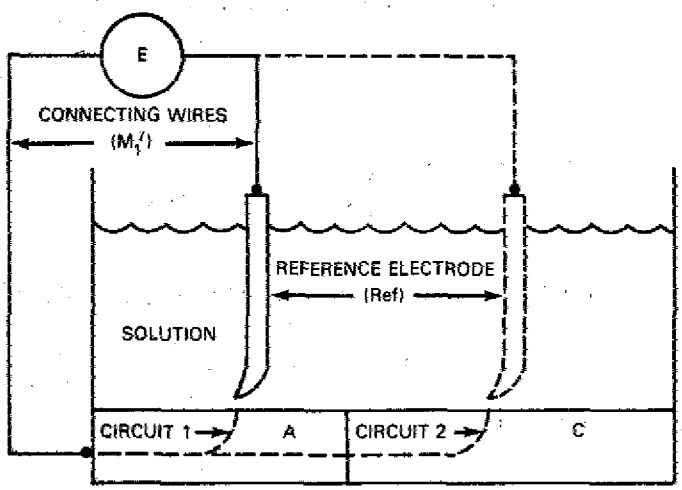

Fig. A1—Method of measuring the electrode potentials of a coplanar anode (A) and cathode (C)

In circuit 1 the measured electrode potential of the anode E_a vs the reference electrode is related to the potential differences across the various interfaces by

$$[\phi_A - P(r, 0)] + [P(r, 0) - \phi_{\text{Ref}}] + (\phi_{\text{Ref}} - \phi_{M_1'}) = E_a, \tag{A1}$$

where ϕ_A is the electrostatic potential "just inside" the metal A and $P(r, 0)$ is the electrostatic potential in the solution "just outside" the metal [A2]. Similarly ϕ_{Ref} and $\phi_{M_1'}$ refer respectively to the electrostatic potential just inside the solid-phase reference electrode and just inside the connecting wire.

According to Bockris and Reddy [A1] the potential difference across a nonpolarizable interface such as ϕ_{Ref}/solution is a constant, so that

$$\phi_A + P(r, 0) - \phi_{\text{Ref}} + (\phi_{\text{Ref}} - \phi_{M_1'}) = V', \tag{A2}$$

where V' is a constant. Use of this definition of V' in Eq. (A1) gives

$$V' - P(r, 0) = E_a, \quad 0 \leqslant r < a. \tag{A3}$$

Similarly measurement of the electrode potential of the cathode E_c in circuit 2 gives

$$(\phi_A - \phi_C) + [\phi_C - P(r, 0)] + [P(r, 0) - \phi_{\text{ref}}] + (\phi_{\text{ref}} - \phi_{M_1'}) = E_c. \tag{A4}$$

The ϕ_C terms in Eq. (A4) cancel, so that

$$V' - P(r, 0) = E_c, \quad a < r \leqslant c. \tag{A5}$$

Thus

$$V' - P(r, 0) = \begin{cases} E_a, & 0 \leqslant r < a \\ E_c, & a < r \leqslant c \end{cases} \tag{A6}$$

Or denoting the electrode potential along the metal surface as $E(r, 0)$ gives

$$V' - P(r, 0) = E(r, 0), \tag{A7}$$

which is Eq. (10) in the main text

REFERENCES

A1. J. O'M. Bockris and A.K.N. Reddy, *Modern Aspects of Electrochemistry*, Vol. 2, Plenum Press, New York, 1970, pp. 644 ff.

A2. D.C. Grahame, *Chem. Revs.* 41, 441 (1947).

Appendix B

COMPUTER PROGRAM FOR COPLANAR CONCENTRIC CIRCULAR ELECTRODES WITH UNEQUAL POLARIZATION PARAMETERS UNDER BULK ELECTROLYTE

```
      PROGRAM UNEQBULK
C
C     THIS PROGRAM COMPUTES
C               (1) CURRENT DISTRIBUTION
C               (2) POTENTIAL DISTRIBUTION
C               (3) TOTAL ANODIC CURRENT
C     FOR CONCENTRIC CIRCULAR ELECTRODES COVERED BY BULK ELECTROLYTE
C     FOR THE CASE WHERE ANODIC AND CATHODIC WAGNER POLARIZATION
C     PARAMETERS ARE NOT EQUAL,
C
C     A=RADIUS OF ANODE
C     C=RADIUS OF CATHODE
C     R=DISTANCE ALONG RADIUS
C     RR=R/C
C     LA=ANODIC WAGNER POLARIZATION PARAMETER
C     LC=CATHODIC WAGNER POLARIZATION PARAMETER
C     X(M)=MTH ZERO OF BESSEL FUNCTION OF ORDER ONE
C     F(R,0)=INTERFACIAL POTENTIAL ALONG THE METAL SURFACE
C     E(R,0)=POTENTL=ELECTRODE POTENTIAL ALONG THE METAL SURFACE
C     E(R,0)=CONSTANT-F(R,0), WITH THE CONSTANT CANCELLING OUT IN THE
C     FINAL EXPRESSION, SO CONSTANT IN EFFECT CAN BE SET EQUAL TO ZERO.
C
C     THE COEFFICIENTS C0 AND CSUBN ARE DEFINED IN THE FOLLOWING EQUATION
C
C                     K
C     F(R,0) = C  + SUM (C  (X(N)*R/C))
C              0   N=1   N 0
C
C     ITOTAL=TOTAL ANODIC CURRENT DIVIDED BY THE CONDUCTIVITY
C     ILOCAL=LOCAL CURRENT DENSITY DIVIDED BY THE CONDUCTIVITY
C
      REAL LA,LC,ITOTAL,ILOCAL
      DIMENSION X(100),Y(100,100),B(100,100)
      PI=3.1415926536
      K=100
    1 READ 10,A,C,LA,LC,EA,EC
   10 FORMAT (6F10.0)
      PRINT 11,A,C,LA,LC,EA,EC
   11 FORMAT (1H1,5X,2HA= F10.5,5X,2HC= F10.5,5X,3HLA= F10.5,5X,3HLC= F1
     10.5,5X,3HEA= F10.5,5X,3HEC= F10.5,////)
      PRINT 12
   12 FORMAT (1X,*GENERATION OF THE SYSTEM OF SIMULTANEOUS EQUATIONS USE
     1D TO SOLVE FOR THE COEFFICIENTS C0 AND CSUBN*,///)
      PRINT 13
   13 FORMAT (1X,*NOT ALL THE COEFFICIENTS SO GENERATED ARE LISTED BELOW
     1*,//)
      PRINT 14
   14 FORMAT (1X,*AS A PARTIAL CHECK, WHEN N=M, THE VALUE OF B(M,N) IS G
     1IVEN BY P*,////)
      PRINT 15
```

```
   15 FORMAT (5X,*M*,9X,*X(M)*,13X,*P*,14X,*Y(M)*,11X,*B(M,1)*,10X,*B(M,
     110)*,9X,*B(M,50)*,8X,*B(M,100)*,//)
C
C     THIS PART OF THE PROGRAM GENERATES THE SYSTEM OF SIMULTANEOUS
C     EQUATIONS USED IN SOLVING FOR THE COEFFICIENTS C0 AND CSUBN.
C
      JORD=1
      NO=K
      CALL BESZERO (JORD,NO,X)
      DO 40 M=1,K
      T1=X(M)/C
      T2=1.0+(LC*T1)
      T3=BESJ(X(M),0)
      T4=(T3**2)/2.0
      T5=T2*T4
      T6=X(M)*A/C
      T7=BESJ(T6,0)
      T8=BESJ(T6,1)
      T9=(T7**2)+(T8**2)
      T10=((LA-LC)*X(M)*((A/C)**2)*T9)/(2.0*C)
      P=T5+T10
   19 Y(M)=-(EA-EC)*(A/C)*(T8/X(M))
      N=1
   20 IF (N.EQ.M) 21,22
   21 B(M,N)=P
      GO TO 30
   22 T12=X(M)/X(N)
      T13=1.0/(1.0-(T12**2))
      T14=X(N)*A/C
      T15=BESJ(T14,1)
      T16=BESJ(T14,0)
      T17=(T15*T7)-(T12*T16*T8)
      B(M,N)=(LA-LC)*(A/(C**2))*T13*T17
      GO TO 30
   30 N=N+1
      IF (N.LE.K) 20,31
   31 PRINT 32,M,X(M),P,Y(M),B(M,1),B(M,10),B(M,50),B(M,100)
   32 FORMAT (3X,I4,7(3X,E13.5))
   40 CONTINUE
C
C     SOLUTION OF THE SYSTEM OF K SIMULTANEOUS EQUATIONS
C     FOR THE COEFFICIENTS CSUBN
C
C     THE SUBROUTINE REPLACES THE CONSTANT VECTORS WITH THE SOLUTION
C     VECTORS.  THUS, THE CONSTANT VECTORS Y(M) DEFINED IN STATEMENT 19
C     ARE REPLACED BY THE SOLUTION VECTORS.  THESE SOLUTION VECTORS
C     ARE LATER RELABELLED AS CSUBN.
C
      CALL MATALG(B,Y,100,100,0,DET,100)
C
```

```
C      CALCULATION OF THE COEFFICIENT CO
C
      PRINT 41
   41 FORMAT (////,1H1,*CALCULATION OF THE COEFFICIENT CO*,//)
      PRINT 42
   42 FORMAT (20X,8HSOLUTION,23X,12H  (X(N)*A/C),4X,4HY(N),12X,14HRUNNIN
     1G SUM OF)
      PRINT 43
   43 FORMAT (20X,7HVECTORS,9X,FHX(N)*A/C,8X,*1*,13X,9H*BESSEL1*,8X,9HTE
     1RMZERO*)
      PRINT 44
   44 FORMAT (5X,*N*,9X,*X(N)*,11X,*Y(N)*,12X,*XNAC*,11X,*BESSEL1*,8X,*T
     1ERMZERO*,10X,*ZTOTAL*,//)
      ZTOTAL=0.0
      DO 46 N=1,K
      XNAC=X(N)*A/C
      BESSEL1=BESJ(XNAC,1)
      TERMZERO=Y(N)*BESSEL1
      ZTOTAL=ZTOTAL+TERMZERO
      PRINT 45,N,X(N),Y(N),XNAC,BESSEL1,TERMZERO,ZTOTAL
   45 FORMAT (3X,I4,6(3X,E13.5))
   46 CONTINUE
      Z1=((A/C)**2)*EA
      Z2=(1.0-((A/C)**2))*EC
      Z3=(A/(C**2))*(2.0*(LA-LC))*ZTOTAL
      PRINT 47,Z1,Z2,Z3
   47 FORMAT (////,5X,3HZ1= E13.5,5X,3HZ2= E13,5,5X,3HZ3= E13,5)
      CO=-Z1-Z2-Z3
      PRINT 48,CO
   48 FORMAT (////,5X,3HCO= E13.5)
C
C      CALCULATION OF THE TOTAL ANODIC CURRENT
C
      PRINT 70
   70 FORMAT (////,1H1,*CALCULATION OF THE TOTAL ANODIC CURRENT*,//)
      PRINT 71
   71 FORMAT (1X,*ITOTAL=TOTAL ANODIC CURRENT DIVIDED BY THE CONDUCTIVIT
     1Y*,//)
      PRINT 72
   72 FORMAT (45X,6HX(N)*A/C,8X,12H  (X(N)*A/C),3X,14H2.0*PI*A*CSUBN)
      PRINT 73
   73 FORMAT (60X,*1*,14X,9H*BESSEL1*)
      PRINT 74
   74 FORMAT (5X,*N*,9X,*X(N)*,11X,*CSUBN*,12X,*XNAC*,10X,*BESSEL1*,9X,*
     1TERMITOT*,9X,*ITOTAL*,//)
      ITOTAL=0.0
      DO 75 N=1,K
      XNAC=X(N)*A/C
      BESSEL1=BESJ(XNAC,1)
      CSUBN=Y(N)
```

```
      TERMITOT=2.0*PI*A*CSUBN*BESSEL1
      ITOTAL=ITOTAL+TERMITOT
      PRINT 75,N,X(N),CSUBN,XNAC,BESSEL1,TERMITOT,ITOTAL
   75 FORMAT (3X,I4,6(3X,E13.5))
   79 CONTINUE
C
C     CALCULATION OF THE LOCAL CURRENT DENSITY
C
      PRINT 80
   80 FORMAT (////,1H1,*CALCULATION OF THE LOCAL CURRENT DENSITY*,//)
      PRINT 81
   81 FORMAT (1X,*ILOCAL=LOCAL CURRENT DENSITY DIVIDED BY THE CONDUCTIVI
     1TY*,///)
  810 READ 811,RCUT
  811 FORMAT (F10.0)
  812 READ 813,RR
  813 FORMAT (F10.0)
      IF (RR.NE.RCUT) 820,90
  820 PRINT 83,RR
   83 FORMAT (////,3X,3HRR= F5.3)
      PRINT 84
   84 FORMAT (45X,6HX(N)*R/C,6X,12H  (X(N)*R/C),3X,16H(1/C)*CSUBN*X(N))
      PRINT 85
   85 FORMAT (60X,*0*,14X,9H*BESSEL2*)
      PRINT 86
   86 FORMAT (5X,*N*,9X,*X(N)*,11X,*CSUBN*,12X,*XNRC*,10X,*BESSEL2*,9X,*
     1TERMILOC*,9X,*ILOCAL*,//)
      ILOCAL=0.0
      DO 89 N=1,K
      XNRC=X(N)*RR
      BESSEL2=BESJ(XNRC,0)
      CSUBN=Y(N)
      TERMILOC=(1.0/C)*CSUBN*X(N)*BESSEL2
      ILOCAL=ILOCAL+TERMILOC
      PRINT 87,N,X(N),CSUBN,XNRC,BESSEL2,TERMILOC,ILOCAL
   87 FORMAT (3X,I4,6(3X,E13.5))
   89 CONTINUE
      GO TO 812
C
C     CALCULATION OF THE POTENTIAL DISTRIBUTION
C     ALONG THE METAL SURFACE
C
   90 PRINT 91
   91 FORMAT (////,1H1,*CALCULATION OF THE POTENTIAL DISTRIBUTION*,//)
      PRINT 92
   92 FORMAT (1X,*POTENTL=E(R,0)=ELECTRODE POTENTIAL ALONG THE METAL SUR
     1FACE*,///)
  920 READ 921,RR
  921 FORMAT (F10.0)
      IF (RR.NE.RCUT) 930,100
```

```
930 PRINT 94,RR
 94 FORMAT (////,3X,3HRR= F5,3)
    PRINT 95
 95 FORMAT (45X,8HX(N)*R/C,6X,12HL (X(N)*R/C),19X,14HRUNNING SUM OF)
    PRINT 96
 96 FORMAT (60X,*0*,13X,14HCSUBN*BESSEL2=,3X,9HTERMPOTL=,7X,12H-C0-SUM
   1POTL*)
    PRINT 97
 97 FORMAT (5X,*N*,9X,*X(N)*,11X,*CSUBN*,12X,*XNRC*,10X,*BESSEL2*,8X,*
   1TERMPOTL*,9X,*SUMPOTL*,9X,*POTENTL*,//)
    SUMPOTL=0.0
    DO 99 N=1,K
    XNRC=X(N)*RR
    BESSEL2=BESJ(XNRC,0)
    CSUBN=Y(N)
    TERMPOTL=CSUBN*BESSEL2
    SUMPOTL=SUMPOTL+TERMPOTL
    POTENTL=-(C0+SUMPOTL)
    PRINT 98,N,X(N),CSUBN,XNRC,BESSEL2,TERMPOTL,SUMPOTL,POTENTL
 98 FORMAT (3X,I4,7(3X,E13,5))
 99 CONTINUE
    GO TO 920
100 END
      SUBROUTINE BESZERO(JORD,NO,ZERO)
C     IDENT NUMBER - C3007R00
C     TITLE - ZEROS OF THE BESSEL FUNCTION OF THE FIRST KIND
C     IDENT NAME - C3-NRL-BESZERO
C     LANGUAGE - 3600/3800 FORTRAN
C     COMPUTER - CDC-3800
C     CONTRIBUTOR - JANET P. MASON, CODE 7813
C                   RESEARCH COMPUTATION CENTER, MIS DIVISION
C     ORGANIZATION - NRL - NAVAL RESEARCH LABORATORY,
C                    WASHINGTON, D.C. 20390
C     DATE - 1 JULY 1971
C     PURPOSE - TO FIND THE FIRST M ZEROS OF JSUBN(X) FOR 0SNS5, WHERE
C               M IS SUPPLIED, BY THE USER, IN THE SUBROUTINE CALL
      DIMENSION XJA0(4),XJA1(3),XJA2(2),XJA3(6),XJA4(6),XJA5(9),ZERO(1)
      DATA(XJA0=2.4048255577,5,5200781103,8,6537279129,11.791534439),
     1    (XJA1=3.8317059702,7,0155866698,10,173468135),
     2    (XJA2=5.1356223,8,4172441),
     3    (XJA3=6.3801619,9,7610231,13,0152007,16.2234640,19,4094148,
     4          22,5827295),
     5    (XJA4=7.5883427,11,0647095,14.3725367,17,6159660,20,8269330,
     6          24,0190195),
     7    (XJA5=8.7714838,12,3386042,15,7001741,18,9801339,22.2177999,
     8          25,4303411,28,6266183,31,8117167,34,9887813)
      PI=3,1415926536
      FOLD=4,0*JORD*JORD
      GO TO (1,2,3,4,5,6)JORD+1
    1 DO 11 I=1,NO
```

```
      IF(I,GT,4)GO TO 20
      ZERO(I)=XJA0(I)
   11 CONTINUE
      RETURN
    2 DO 12 I=1,NO
      IF(I,GT,3)GO TO 20
      ZERO(I)=XJA1(I)
   12 CONTINUE
      RETURN
    3 DO 13 I=1,NO
      IF(I,GT,2)GO TO 20
      ZERO(I)=XJA2(I)
   13 CONTINUE
      RETURN
    4 DO 14 I=1,NO
      IF(I,GT,6)GO TO 20
      ZERO(I)=XJA3(I)
   14 CONTINUE
      RETURN
    5 DO 15 I=1,NO
      IF(I,GT,6)GO TO 20
      ZERO(I)=XJA4(I)
   15 CONTINUE
      RETURN
    6 DO 16 I=1,NO
      IF(I,GT,9)GO TO 20
      ZERO(I)=XJA5(I)
   16 CONTINUE
      RETURN
   20 BETA=(PI/4,0)*(2,0*JORD+4,0*I-1,0)
      W1=BETA*8.0
      W2=W1*W1
      ZERO(I)=BETA-(HOLD-1,0)/W1*(1,0+1.0/W2*(4,0*(7,0*HOLD-31,0)/3,0
     1      +1,0/W2*(32,0*(83,0*HOLD*HOLD-982,0*HOLD+3779,0)/15,0
     2      +1,0/W2*(64,0*(6949,0*HOLD*HOLD*HOLD-153855,0*HOLD*HOLD
     3      +1585743,0*HOLD-6277237,0)/105,0))))
      GO TO (11,12,13,14,15,16),JORD+1
   10 END
      FUNCTION BESJ(X,N)
      DATA(R0=,2827844947E8),(R1=-,6652659891E7),(R2=.3883131226E6),
     1(R3=-,9057867427E4),(R4=,1083069683E3),(R5=-,7348533593E5),
     2(R6=,2921267248E-2),(R7=-,6505017057E-5),(R8=.6453801805E-8),
     3(S0=,2827844947E8),(S1=,2169524774E6),(S2=,7004682514E3),
     4(A0=2,5323420902E2),(A1=4,2217704118E1),(A2=5,2443314672E-1),
     5(B0=,4488459489E3),(B1=,7532204857E2),
     6(C0=-1,2339445551E1),(C1=-2,7768921059),(C2=-4,9517399126E-2),
     7(D1=,4100554523E2),(F=64,),(G=4,7225664852 1),
     8(D0=,1749687823E3),
     A(RR0=.9808727495E7),(RR1=-,1142532572E7),(RR2=,4094621362E5),
     B(RR3=-,6666011985E3),(RR4=,5757541403E1),(RR5=-,2790447551E-1),
```

```
      C(RR6=,73493132111E-4),(RR7=-,84306821641E+7),
      D(SS0=,19617454991E8),(SS1=,16711673184E6),(SS2=.60777258247E3),
      E(RB0=,62836856631E3),(BB1=,97300094628E2),
      F(DD0=,21185478331E3),(DD1=,46517127629E2),
      G(AA0=3,5451899975E2),(AA1=5,5544843021E1),(AA2=6,5223084285E-1),
      H(CC0=4,4822348226E1),(CC1=9,7348068764),(CC2=1,7725579145E-1)
      D=X*X
      IF(N,EQ,0) GO TO 6 $ IF(N,EQ,1) GO TO 7 $ GO TO 8
    6 IF(D-F)1,1,2
    1 P=((((R8*D+R7)*D+R6)*D+R5)*D+R4)*D $ P=(((P+R3)*D+R2)*D+R1)*D+R0
      BESJ =P/(((D+S2)*D+S1)*D+S0) $ RETURN
    2 IF(D,GT,G) GO TO 9
      A=ABS(X) $ D=F/D
      P=((A2*D+A1)*D+A0)/((D+B1)*D+B0)
      C=  ((C2*D+C1)*D+C0)/(A*((D+D1)*D+D0))
      BESJ =(COS(A)*(P+C)+SIN(A)*(P-C))/SQRT(A)
      RETURN
    7 IF(D-F)11,11,21
   11 P=((((((RR7*D+RR6)*D+RR5)*D+RR4)*D+RR3)*D+RR2)*D+RR1)*D+RR0
      BESJ=X*P/(((D+SS2)*D+SS1)*D+SS0) $ RETURN
   21 IF(D,GT,G) GO TO 9
      A=ABS(X) $ D=F/D
      P=((AA2*D+AA1)*D+AA0)/((D+BB1)*D+BB0)
      C=((CC2*D+CC1)*D+CC0)/(A*((D+DD1)*D+DD0))
      A=( COS(A)*(C-P)+SIN(A)*(C+P))/SQRT(A) $ IF(X,LT,0)A=-A
      BESJ=A
      RETURN
    8 PRINT 81,N
   81 FORMAT(//15X*ERROR IN BESJ, N =*I5)
      GO TO 100
    9 PRINT91,X
   91 FORMAT(//15X*ERROR IN BESJ, ARGUMENT X TOO LARGE, X = *E17,10)
  100 BESJ=1,E300
      END
      SUBROUTINE MATALG(A,X,NR,NV,IDG,DET,NACT)
      DIMENSION A(NACT,NACT),X(NACT,NACT)
      IF(IDG) 1,2,1
    1 DO 3 I=1,NR
      DO 4 J=1,NR
    4 X(I,J)=0,0
    3 X(I,I)=1,0
      NV=NR
    2 DET=1.0
      NR1=NR-1
      DO 5 K=1,NR1
      IP1=K+1
      PIVOT=0,0
      DO 6 I=K,NR
      Z=ABSF(A(I,K))
      IF(Z-PIVOT) 6,6,7
```

```
  7 PIVØT=Z
    IPR=I
  6 CONTINUE
    IF(PIVØT) 8,9,8
  9 DET=0.0
    RETURN
  8 IF(IPR-K) 10,11,10
 10 DØ 12 J=K,NR
    Z=A(IPR,J)
    A(IPR,J)=A(K,J)
 12 A(K,J)=Z
    DØ 13 J=1,NV
    Z=X(IPR,J)
    X(IPR,J)=X(K,J)
 13 X(K,J)=Z
    DET=-DET
 11 DET=DET*A(K,K)
    PIVØT=1.0/A(K,K)
    DØ 14 J=IR1,NR
    A(K,J)=A(K,J)*PIVØT
    DØ 14 I=IR1,NR
 14 A(I,J)=A(I,J)-A(I,K)*A(K,J)
    DØ 5 J=1,NV
    IF(X(K,J)) 15,5,15
 15 X(K,J)=X(K,J)*PIVØT
    DØ 16 I=IR1,NR
 16 X(I,J)=X(I,J)-A(I,K)*X(K,J)
  5 CONTINUE
    IF(A(NR,NR)) 17,9,17
 17 DET=DET*A(NR,NR)
    PIVØT=1.0/A(NR,NR)
    DØ 18 J=1,NV
    X(NR,J)=X(NR,J)*PIVØT
    DØ 18 K=1,NR1
    I=NR-K
    SUM=0.0
    DØ 19 L=I,NR1
 19 SUM=SUM+A(I,L+1)*X(L+1,J)
 18 X(I,J)=X(I,J)-SUM
    END
```

Appendix C

COMPUTER PROGRAM FOR COPLANAR CONCENTRIC CIRCULAR ELECTRODES WITH UNEQUAL POLARIZATION PARAMETERS UNDER THIN-LAYER ELECTROLYTE

```
      PROGRAM UNEQTHIN
C
C     THIS PROGRAM COMPUTES
C               (1) CURRENT DISTRIBUTION
C               (2) POTENTIAL DISTRIBUTION
C               (3) TOTAL ANODIC CURRENT
C     FOR CONCENTRIC CIRCULAR ELECTRODES COVERED BY THIN-LAYER ELECTROLYTE
C     FOR THE CASE WHERE ANODIC AND CATHODIC WAGNER POLARIZATION
C     PARAMETERS ARE NOT EQUAL.
C
C     A=RADIUS OF ANODE
C     C=RADIUS OF CATHODE
C     R=DISTANCE ALONG RADIUS
C     BLENGTH=THICKNESS OF ELECTROLYTE LAYER
C     RR=R/C
C     LA=ANODIC WAGNER POLARIZATION PARAMETER
C     LC=CATHODIC WAGNER POLARIZATION PARAMETER
C     X(M)=MTH ZERO OF BESSEL FUNCTION OF ORDER ZERO
C     P(R,0)=INTERFACIAL POTENTIAL ALONG THE METAL SURFACE
C     E(R,0)=POTENTL=ELECTRODE POTENTIAL ALONG THE METAL SURFACE
C     E(R,0)=CONSTANT-P(R,0), WITH THE CONSTANT CANCELLING OUT IN THE
C     FINAL EXPRESSION, SO CONSTANT IN EFFECT CAN BE SET EQUAL TO ZERO.
C
C     THE COEFFICIENTS CO AND CSUBN ARE DEFINED IN THE FOLLOWING EQUATION
C
C                       M
C     P(R,0) = C  + SUM (C  . (X(N)*R/C))
C               0   N=1   N 0
C
C     ITOTAL=TOTAL ANODIC CURRENT DIVIDED BY THE CONDUCTIVITY
C     ILOCAL=LOCAL CURRENT DENSITY DIVIDED BY THE CONDUCTIVITY
C
      REAL LA,LC,ITOTAL,ILOCAL
      DIMENSION X(100),Y(100,100),B(100,100)
      PI=3,1415926536
      M=100
    1 READ 10,A,C,BLENGTH,LA,LC,EA,EC
   10 FORMAT (7F10,0)
      PRINT 11,A,C,BLENGTH,LA,LC,EA,EC
   11 FORMAT (1H1,5X,2HA= F10.5,5X,2HC= F10,5,5X,8HBLENGTH= F10.5,5X,3HL
     1A= F10,5,5X,3HLC= F10,5,5X,3HEA= F10.5,5X,3HEC= F10.5,////)
      PRINT 12
   12 FORMAT (1X,*GENERATION OF THE SYSTEM OF SIMULTANEOUS EQUATIONS USE
     1D TO SOLVE FOR THE COEFFICIENTS CO AND CSUBN*,///)
      PRINT 13
   13 FORMAT (1X,*NOT ALL THE COEFFICIENTS SO GENERATED ARE LISTED BELOW
     1*,//)
      PRINT 14
   14 FORMAT (1X,*AS A PARTIAL CHECK, WHEN N=M, THE VALUE OF B(M,N) IS G
     1IVEN BY P*,////)
```

```
      PRINT 15
   15 FORMAT (5X,*M*,9X,*X(M)*,13X,*F*,14X,*Y(M)*,11X,*B(M,1)*,10X,*B(M,
     110)*,9X,*B(M,50)*,8X,*B(M,100)*,//)
C
C     THIS PART OF THE PROGRAM GENERATES THE SYSTEM OF SIMULTANEOUS
C     EQUATIONS USED IN SOLVING FOR THE COEFFICIENTS CO AND CSUBN,
C
      JORD=1
      NE=K
      CALL BESZERO (JORD,NE,X)
      DO 40 M=1,K
      XMBC=X(M)*BLENGTH/C
      SINHXMBC=(EXP(XMBC)-EXP(-XMBC))/2.0
      COSHXMBC=(EXP(XMBC)+EXP(-XMBC))/2.0
      TANHXMBC=SINHXMBC/COSHXMBC
      T1=X(M)/C
      T2=1.0+(LC*T1*TANHXMBC)
      T3=BESJ(X(M),0)
      T4=(T3**2)/2.0
      T5=T2*T4
      T6=X(M)*A/C
      T7=BESJ(T6,0)
      T8=BESJ(T6,1)
      T9=(T7**2)+(T8**2)
      T10=((LA-LC)*X(M)*((A/C)**2)*T9*TANHXMBC)/(2.0*C)
      F=T5+T10
   19 Y(M)=-(1.0/COSHXMBC)*(EA-EC)*(A/C)*(T8/X(M))
      N=1
   20 IF (N.EQ.M) 21,22
   21 B(M,N)=F
      GO TO 30
   22 T12=X(M)/X(N)
      T13=1.0/(1.0-(T12**2))
      T14=X(N)*A/C
      T15=BESJ(T14,1)
      T16=BESJ(T14,0)
      T17=(T15*T7)-(T12*T16*T8)
      XNBC=X(N)*BLENGTH/C
      SINHXNBC=(EXP(XNBC)-EXP(-XNBC))/2.0
      B(M,N)=(LA-LC)*(A/(C**2))*(1.0/COSHXMBC)*T13*T17*SINHXNBC
      GO TO 30
   30 N=N+1
      IF (N.LE.K) 20,31
   31 PRINT 32,M,X(M),F,Y(M),B(M,1),B(M,10),B(M,50),B(M,100)
   32 FORMAT (3X,I4,7(3X,E13.5))
   40 CONTINUE
C
C     SOLUTION OF THE SYSTEM OF K SIMULTANEOUS EQUATIONS
C     FOR THE COEFFICIENTS CSUBN
C
```

```
C     THE SUBROUTINE REPLACES THE CONSTANT VECTORS WITH THE SOLUTION
C     VECTORS.  THUS, THE CONSTANT VECTORS Y(M) DEFINED IN STATEMENT 19
C     ARE REPLACED BY THE SOLUTION VECTORS.  THESE SOLUTION VECTORS
C     ARE LATER RELABELLED AS CSUBN.
C
      CALL MATALG(B,Y,100,100,0,DET,100)
C
C     CALCULATION OF THE COEFFICIENT CO
C
      PRINT 41
   41 FORMAT (////,1H1,*CALCULATION OF THE COEFFICIENT CO*,//)
      PRINT 42
   42 FORMAT (28X,8HSOLUTION,23X,12H  (X(N)*A/C),2X,10HSINH(X(N)*,7X,13H
     1Y(N)*SINHXNBC,3X,14HRUNNING SUM OF)
      PRINT 43
   43 FORMAT (28X,7HVECTORS,9X,8HX(N)*A/C,8X,*1*,17X,10HBLENGTH/C),2X,9H
     1*BESSEL1*,7X,9HTERMZERO*)
      PRINT 44
   44 FORMAT (5X,*N*,9X,*X(N)*,11X,*Y(N)*,12X,*XNAC*,11X,*BESSEL1*,9X,*S
     1INHXNBC*,7X,*TERMZERO*,10X,*ZTOTAL*,//)
      ZTOTAL=0.0
      DO 46 N=1,K
      XNAC=X(N)*A/C
      BESSEL1=BESJ(XNAC,1)
      XNBC=X(N)*BLENGTH/C
      SINHXNBC=(EXP(XNBC)-EXP(-XNBC))/2.0
      TERMZERO=Y(N)*BESSEL1*SINHXNBC
      ZTOTAL=ZTOTAL+TERMZERO
      PRINT 45,N,X(N),Y(N),XNAC,BESSEL1,SINHXNBC,TERMZERO,ZTOTAL
   45 FORMAT (3X,I4,7(3X,E13.5))
   46 CONTINUE
      Z1=((A/C)**2)*EA
      Z2=(1.0-((A/C)**2))*EC
      Z3=(A/(C**2))*(2.0*(LA-LC))*ZTOTAL
      PRINT 47,Z1,Z2,Z3
   47 FORMAT (////,5X,3HZ1= E13.5,5X,3HZ2= E13.5,5X,3HZ3= E13.5)
      CO=-Z1-Z2-Z3
      PRINT 48,CO
   48 FORMAT (////,5X,3HCO= E13.5)
C
C     CALCULATION OF THE TOTAL ANODIC CURRENT
C
      PRINT 70
   70 FORMAT (////,1H1,*CALCULATION OF THE TOTAL ANODIC CURRENT*,//)
      PRINT 71
   71 FORMAT (1X,*ITOTAL=TOTAL ANODIC CURRENT DIVIDED BY THE CONDUCTIVIT
     1Y*,//)
      PRINT 72
   72 FORMAT (45X,8HX(N)*A/C,6X,12H  (X(N)*A/C),2X,10HSINH(X(N)*,7X,14H2
     1.0*PI*A*CSUBN)
```

```
      PRINT 73
   73 FORMAT (60X,*1*,17X,10HBLENGTH/C),2X,17H*SINHXNBC*BESSEL1)
      PRINT 74
   74 FORMAT (5X,*N*,9X,*X(N)*,11X,*CSUBN*,11X,*XNAC*,11X,*BESSEL1*,9X,*
     1SINHXNBC*,7X,**TERMITOT*,9X,*ITOTAL*,//)
      ITOTAL=0,0
      DO 79 N=1,K
      XNAC=X(N)*A/C
      BESSEL1=BESJ(XNAC,1)
      CSUBN=Y(N)
      XNBC=X(N)*BLENGTH/C
      SINHXNBC=(EXP(XNBC)-EXP(-XNBC))/2.0
      TERMITOT=2,0*PI*A*CSUBN*BESSEL1*SINHXNBC
      ITOTAL=ITOTAL+TERMITOT
      PRINT 75,N,X(N),CSUBN,XNAC,BESSEL1,SINHXNBC,TERMITOT,ITOTAL
   75 FORMAT (3X,I4,7(3X,E13,5))
   79 CONTINUE
C
C     CALCULATION OF THE LOCAL CURRENT DENSITY
C
      PRINT 80
   80 FORMAT (////,1H1,*CALCULATION OF THE LOCAL CURRENT DENSITY*,//)
      PRINT 81
   81 FORMAT (1X,*ILOCAL=LOCAL CURRENT DENSITY DIVIDED BY THE CONDUCTIVI
     1TY*,///)
  810 READ 811,RCUT
  811 FORMAT (F10.0)
  812 READ 813,RR
  813 FORMAT (F10.0)
      IF (RR,NE.RCUT) 820,90
  820 PRINT 83,RR
   83 FORMAT (////,3X,3HRR= F5,3)
      PRINT 84
   84 FORMAT (45X,8HX(N)*R/C,6X,12HJ (X(N)*R/C),2X,10HSINH(X(N)*,7X,16H(
     11/C)*CSUBN*X(N))
      PRINT 85
   85 FORMAT (60X,*0*,17X,10HBLENGTH/C),2X,17H*SINHXNBC*BESSEL2)
      PRINT 86
   86 FORMAT (5X,*N*,9X,*X(N)*,11X,*CSUBN*,12X,*XNRC*,10X,*BESSEL2*,9X,*
     1SINHXNBC*,7X,**TERMILOC*,9X,*ILOCAL*,//)
      ILOCAL=0,0
      DO 89 N=1,K
      XNRC=X(N)*RR
      BESSEL2=BESJ(XNRC,0)
      CSUBN=Y(N)
      XNBC=X(N)*BLENGTH/C
      SINHXNBC=(EXP(XNBC)-EXP(=XNBC))/2.0
      TERMILOC=(1.0/C)*CSUBN*X(N)*SINHXNBC*BESSEL2
      ILOCAL=ILOCAL+TERMILOC
      PRINT 87,N,X(N),CSUBN,XNRC,BESSEL2,SINHXNRC,TERMILOC,ILOCAL
```

```
   87 FORMAT (3X,I4,7(3X,E13.5))
   89 CONTINUE
      GO TO 812
C
C     CALCULATION OF THE POTENTIAL DISTRIBUTION
C     ALONG THE METAL SURFACE
C
   90 PRINT 91
   91 FORMAT (////,1H1,*CALCULATION OF THE POTENTIAL DISTRIBUTION*,//)
      PRINT 92
   92 FORMAT (1X,*POTENTL=E(R,0)=ELECTRODE POTENTIAL ALONG THE METAL SUR
     1FACE*,///)
  920 READ 921,RR
  921 FORMAT (F10.0)
      IF (RR.NE.RCUT) 930,100
  930 PRINT 94,RR
   94 FORMAT (////,3X,3HRR= F5.3)
      PRINT 95
   95 FORMAT (43X,12HJ (X(N)*R/C),2X,10HCOSH(X(N)*,7X,13HCSUBN*BESSEL2,3
     1X,14HRUNNING SUM OF)
      PRINT 96
   96 FORMAT (44X,*0*,17X,10HBLENGTH/C),3X,10H*COSHXNBC*,6X,9HTERMPOTL*,
     16X,12H-C0-SUMPOTL*)
      PRINT 97
   97 FORMAT (5X,*N*,9X,*X(N)*,11X,*CSUBN*,10X,*BESSEL2*,9X,*COSHXNBC*,8
     1X,*TERMPOTL*,8X,*SUMPOTL*,8X,*POTENTL*,//)
      SUMPOTL=0.0
      DO 99 N=1,K
      XNRC=X(N)*RR
      BESSEL2=BESJ(XNRC,0)
      CSUBN=Y(N)
      XNBC=X(N)*BLENGTH/C
      COSHXNBC=(EXP(XNBC)+EXP(-XNBC))/2.0
      TERMPOTL=CSUBN*BESSEL2*COSHXNBC
      SUMPOTL=SUMPOTL+TERMPOTL
      POTENTL=-(CJ+SUMPOTL)
      PRINT 98,N,X(N),CSUBN,BESSEL2,COSHXNBC,TERMPOTL,SUMPOTL,POTENTL
   98 FORMAT (3X,I4,7(3X,E13.5))
   99 CONTINUE
      GO TO 920
  100 END
```

SUBROUTINES BESZERO (JORD, NO, ZERO), FUNCTION BESJ (X, N), AND MATALG (A, X, NR, NV, IDO, DET, NACT) ARE GIVEN IN APPENDIX B.

U.S. GOVERNMENT PRINTING OFFICE: 1977 240-824/142 1-3